Studies of N-Terminal Templates for α-Helix Formation. Synthesis and Conformational Analysis of Peptide Conjugates of (2S,5S,8S,11S)-1-Acetyl-1,4-diaza-3-keto-5-carboxy-10-thiatricyclo[2.8.1.0^{4,8}]-tridecane (Ac-Hel$_1$-OH)

D. S. Kemp,* Timothy P. Curran, James G. Boyd, and Thomas J. Allen

Room 18-582, Department of Chemistry, Massachusetts Institute of Technology, Cambridge, Massachusetts 02139

Received January 23, 1991 (Revised Manuscript Received July 1, 1991)

The following peptide conjugates of the above-named template molecule were prepared: Ac-Hel$_1$-(L-Ala)$_n$-OtBu (n = 1–6) and Ac-Hel$_1$-Sar-(L-Ala)$_n$-OtBu (n = 1–4), where Sar = *N*-methylglycine. The slowly equilibrating acetamido function causes the ^{1}H NMR spectrum in $CDCl_3$, CD_3CN, DMF-d_7, and DMSO-d_6 to be split into pairs of resonances corresponding to the s-cis (c) and s-trans (t) amide conformations. The (t)/(c) ratio is formed to be length and solvent dependent for the homoAla oligomers, and the pattern of resonances in the δ 2–3 region of these conjugates is shown to be consistent with a change in conformation at the C-8–C-9 bond concurrent with length-dependent (t) state formation. Study of NOE properties, temperature and solvent dependences of NH chemical shifts, and $J_{\alpha CH-NH}$ values are shown to be consistent with an assignment of random coil conformations for the (c) states and template-nucleated helical conformations for the (t) states. Solvent-dependent helicity propagation parameters are assigned.

A helix-coil transition[1] of a macromolecule is a dramatic example of order created out of chaos. Acting within an initially amorphous but order-susceptible region of a linear polymer, a conformational signal arising from a linked, locally structured region replicates a specific structural motif. Conformational signaling and replication provide

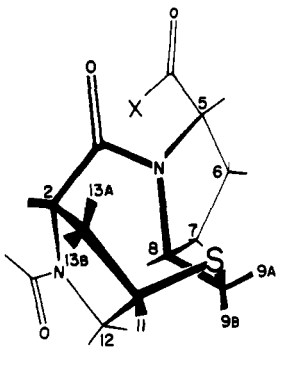

1a

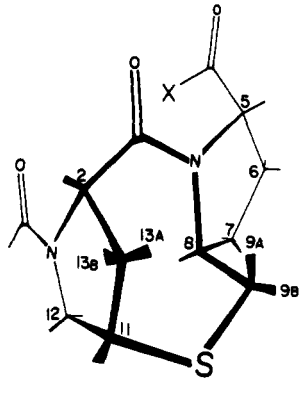

1b

fertile topics for synthetic or bioorganic chemists who wish to generalize the folding patterns of the well-known biopolymers to a broader range of macromolecules. In this paper we report a study of helical order induction in a polypeptide chain by means of a linked N-terminal region that has an ordered conformation with helical hydrogen bonding sites that can transmit conformational information. Using ^{1}H NMR spectroscopy we now examine the conformational properties of conjugates of **1** with alanine oligomers in the organic solvents $CDCl_3$, CD_3CN, DMF-d_7, and DMSO-d_6 to determine whether **1** in fact acts as a conformational template for helix formation. The important topic of helix nucleation in water will be addressed in subsequent reports.

(1) Poland, D.; Scheraga, H. A. Statistical Mechanical Theory of Order-Disorder Transitions in Biological Macromolecules; Academic Press: New York, 1970. Zimm, B. H.; Bragg, J. K. *J. Chem. Phys.* **1959**, *31*, 526–535.

Reporter Properties of the Template

We define a *conformational template* as a structure-communicating functionality that acts under favorable conditions to enforce a single conformation on a linked chain of atoms that is normally conformationally inhomogeneous. A first feasibility study of conformational templates should involve a linear molecule for which initiation of the desired conformation is relatively difficult, ensuring the relevance of the template, and in which the ease of propagation of the conformation is highly sensitive to external variables, allowing study of growth of ordered structures under a range of progressively less favorable conditions. By both criteria the α-helical conformation of linear polypeptides is ideal.

The accompanying paper reports the synthesis of a potential helical template for linked peptides. In the crystal and in $CDCl_3$ solution this template as the free acid was shown to exist as the (cs) conformation **1a** (X = OH). Peptide conjugates with this template conformation cannot accomodate an intramolecular hydrogen bond to the acetamido carbonyl and are expected to be nonhelical. In solution in other solvents the acid exists as a mixture of (cs) and (ts) conformations that differ only by the orientation of the acetamido function and that equilibrate slowly on the NMR time scale, owing to slow rotation at the C–N amide bond. Molecular mechanics calculations suggest that the (te) conformation **1b** (X = OH) in which the thiamethylene group has also reoriented must be only slightly less stable than the (ts). Equilibration between (s) and (e) states is expected to be rapid on the NMR time scale, resulting in NMR properties for (t) resonances that are (s)–(e) state averages. Calculations also imply that the (te) state has three properly oriented hydrogen-bonding sites and should be capable of efficient nucleation of helices in linked polypeptides. The (ts) state forms intramolecular hydrogen bonds to the acetamido oxygen that are 0.1–0.3 Å longer than those formed by the (te) state; it is thus expected to be substantially less efficient at helical nucleation. The fourth state (ce) is nonnucleating and is also predicted to be less stable. This state has not been observed.

0022-3263/91/1956-6683$02.50/0

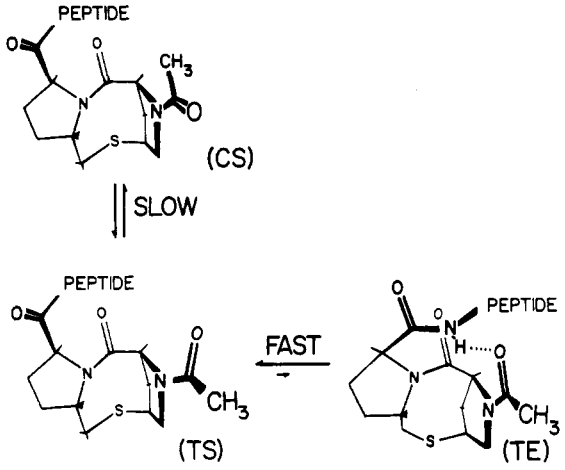

Figure 1. Conformational substrates of the Ac-Hel$_1$-peptide conjugates. The nonhelical (cs) state equilibrates in minutes to seconds with a nonhelical (ts) state which is in very rapid equilibrium with a succession of (te) states, one for each NH of the peptide backbone.

The slowly equilibrating cis–trans acetamido conformers appear in NMR spectra as pairs of resonances, with relative areas corresponding to the ratio of (t)/(c) state abundances. The NMR properties of each resonance are abundance-weighted averages over all rapidly equilibrating conformations that contribute to the (c) or (t) state. Since the (cs) state is incapable of helix nucleation, provided no other length-dependent structure is nucleated from the template region, its stability must reflect the average properties of the nonhelical peptide and can be used as an energetic reference. Provided helical nucleation occurs at the template–peptide interface of the (te) state, the (t)/(c) state ratio is directly related to helical stability. Increased helical character of a peptide–template conjugate should then be signaled in two ways: by an increase in this ratio as measured by relatively peak areas, and, within the (t) state, by a shift in the (ts)–(te) state average, reflected by changes in chemical shifts and coupling constants for (t) state resonances. This situation is summarized schematically in Figure 1.

As noted in the accompanying paper, assignment of resonances as (t) or (c) states is facilitated by 2D COSY and ROESY spectra. A preliminary assignment can be made from resonances of the C-12 protons, which appear at δ 3.83 for the s-cis (c) state in $CDCl_3$, and at δ 3.82 (s-cis) (c) and δ 4.00 (s-trans) (t) in D_2O, with similar chemical shifts in other solvents. As evident from **1ab**, within the (t) state manifold, changes in relative weightings of the (ts) and (te) states should be signaled by chemical shift changes for the resonances belonging to the protons at C-9 and C-13 and by changes in the vicinal coupling constants at the C_8–C_9 bond. A relatively pure (ts) state is expected to exhibit a strong NOE between a proton at C-12 and the b-proton at C-9; a nearly pure (te) state should exhibit a strong NOE between the protons at C-9a and C-13a.

Background

The time scale in solution for the formation of helical structures and presumably for the interconversion of helical substates is measured in microseconds, ensuring that kinetics is not an important issue for the study of templated helices.[2]

Equilibrium models for the propagation of order along the backbone of a linear molecule usually involve an initiation parameter σ, which reflects the difficulty of generating a particular conformation at a normal chain locus, and a propagation parameter s, which reflects the ease of growth of order from that structured site.[1] Since the observation by Doty and co-workers that certain oligopeptides of high molecular weight undergo length-dependent helix formation under a variety of solvent conditions,[3] abundant experimental and theoretical information has accumulated for this system, and an analysis by Scheraga and co-workers of helical nucleation of host–guest oligopeptides in water has established that the Zimm–Bragg initiation parameter σ is typically 10^{-3} and the propagation parameter s for helix-favoring amino acid residues is only slightly larger than unity for these high molecular weight systems.[4] For helices of moderate length n, the fraction of helical states is roughly proportional to σs^{n-2},[1] and these results are therefore consistent with many early reports of the failure of short peptides to assume helical conformations in water.[5]

Early studies of oligopeptides demonstrated that helices are strongly stabilized in relatively nonpolar aprotic solvents such as chloroform and strongly destabilized in aggressively hydrogen bond donating solvents like dichloroacetic or trifluoroacetic acid or hydrogen bond accepting solvents like DMSO.[6] A plausible interpretation is that s for an α-helix is dependent upon the relative stabilities of hydrogen bonds between amide residues within the helix and competing hydrogen bonds between backbone amides and solvent molecules. The explanation for the potent helix-stabilizing effect in water by even small volume percentages of the fluorinated alcohol trifluoroethanol is unclear.[7]

The early models based on oligopeptide properties made no allowance for electrostatic interactions involving the helix dipole or between side-chain functions, and the importance of these has been recently emphasized,[8] particularly by Baldwin and co-workers, who have carried out a detailed structure–function analysis of the unusual helical stability exhibited at low temperatures in water by the S- and C-peptide of RNase and their analogues.[7] From such studies Baldwin and Marqusee[9] have recently been led to question the relevance for small peptides of the aqueous s values of 1.06 obtained for alanine from host–guest macromolecular studies.[4] An issue of this kind can be resolved by a study of templated helices, and a report of our own study of this problem is published elsewhere.[10]

The classical Pauling–Corey α-helix is an idealization that lacks the discontinuity of end groups. To establish the preferred structures of short helices, one must turn to statistical analysis of X-ray crystallographic data for helical proteins and peptides. Helices in myoglobin[11] and lysozyme terminate frequently in 3_{10}-α helical composites, and

(2) Schwartz, G. *J. Mol. Biol.* **1965**, *15*, 284–297.

(3) Doty, P.; Wada, A.; Yang, J. T.; Blout, E. *J. Polymer Sci.* **1957**, *23*, 851.

(4) Scheraga, H. A. *Pure Appl. Chem.* **1978**, *50*, 315. Vasquez, M.; Pincus, M. R.; Scheraga, H. A. *Biopolymers* **1987**, *26*, 351–371.

(5) Lotun, N.; Berger, A.; Katchalski, E. *Ann. Rev. Biochem.* **1972**, *41*, 869. Goodman, M.; Langsam, M.; Rosen, I. G. *Biopolymers* **1966**, *4*, 305.

(6) Fasman, G. D. In *Polyamino Acids—Protein Models for Conformational Studies*; Fasman, G. D., Ed.; M. Dekker: 1967; Vol. 1, pp 510–533. Goodman, M.; Verdini, A. S.; Toniolo, C.; Phillips, W. D.; Bovey, F. A. *Proc. Nat. Acad. Sci. U.S.A.* **1969**, *64*, 444.

(7) Bierzynski, A.; Kim, P. S.; Baldwin, R. L. **1982**, *79*, 2470–2474. Kim, P. S.; Bierzynski, A.; Baldwin, R. L. *J. Mol. Biol.* **1982**, *162*, 187–199.

(8) Scheraga, H. *Proc. Nat. Acad. Sci. U.S.A.* **1985**, *82*, 5585–5587.

(9) Marqusee, S.; Baldwin, R. L. *Proc. Nat. Acad. Sci. U.S.A.* **1989**, *86*, 5286.

(10) Kemp, D. S.; Boyd, J. G.; Muendel, C. C. *Nature* **1991**, *352*, 451–454.

(11) Watson, H. C. *Prog. Stereochem.* **1969**, *4*, 305–306.

Nemethy, Phillips, Leach, and Scheraga noted that these end-group deviations are consistent with an alternative choice of ϕ,ψ angles and a new α_{II} helical structure containing bifurcated hydrogen bonds.[12] In an extensive series of X-ray structural analyses of crystalline small peptides constaining helix-favoring Aib (α-aminoisobutyric acid) residues, Karle has noted that hybrid 3_{10}-α helical structures are common among these,[13] as well as hydrated helices in which a water molecule is interdigitated within a loop of a helix.[14] A decapeptide Boc-W-I-A-Aib-I-V-Aib-L-Aib-P-OMe has been found to assume two crystal forms, one described by the 3_{10} helical conformation and the other as an α-helix, yet in neither are there lateral intermolecular hydrogen bonds or close van der Waals interactions that might result in large intermolecular deformations.[15] Structural variability is thus common for short helices, and 3_{10} and α-helices appear in these cases to be comparable in stability. Marshall has used calculational models to arrive at a similar conclusion.[16]

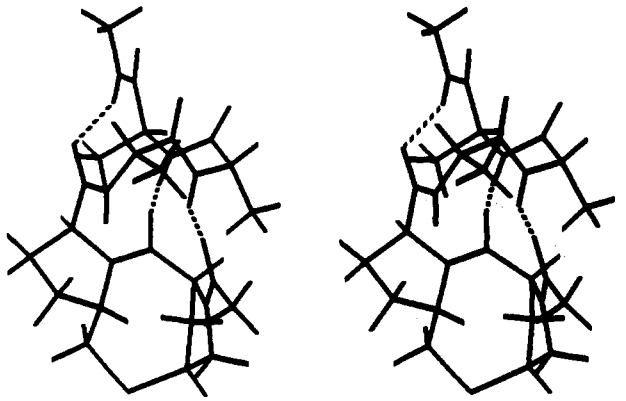

2

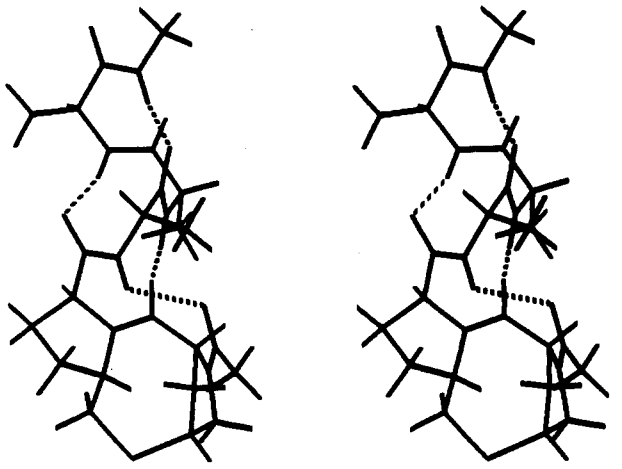

3

Since the template 1 provides only three amide carbonyls as basic sites for hydrogen bonds, it can potentially nucleate helices that are 3_{10}, α, or hybrids of the two. Representation of peptide conjugates of 1 in α-helical and 3_{10}-helical conformations are shown in **2** and **3**, and comparison of these structures reveals that for a pure α-helix to form, the amide NH of the peptide residue adjacent to the template 1 must forgo intramolecular hydrogen bonding. Formation of a pure α-helix is thus most likely in a solvent that is a strong hydrogen bond acceptor that can stabilize the proximal NH, or with peptide analogues that lack a secondary amide function at the template junction.

Scope and Special Features of This Study

The two essential points to be demonstrated by this study are as follows: (1) that in appropriate solvents the template 1 nucleates helices in linked polypeptides, and (2) that the resulting structure exhibits end-to-end communication, so that changes in either the template or the distal end of the peptide have detectable conformational effects throughout the conjugate. Before considering the data pertinent to these points, it is necessary to examine the interaction between solvent-dependent s values and the composition of the substates whose averages yield the experimentally observed (t) state NMR parameters.

Two limiting cases can be profitably considered that follow from the analysis of the Appendix. In a solvent for which the s value is large (say, >2), the most abundant helical state is that in which all amino acid residues have a helical orientation, as noted in Table I. Following the analysis of Figure 1 one sees that this (te_n) state must be substantially more stable than the nonnucleating (ts) state or any other (te) state. In this robust helical case, the (t) state NMR resonances are dominated by properties of the limiting all-helical structure, and the (t)/(c) ratio is very large.

In a solvent for which s is close to 1, the nucleated helix must be frayed unidirectionally, all helical substates are of similar stability, and the (t) state resonances are averages over n (te) states and the nonhelical (ts) state. The influence of the latter should be diluted by the contributions of multiple (te) states as n increases, resulting in a convergence of NMR (t)-state template NMR parameters to limiting helical values with n sufficiently large.

As noted in Figure 2, frayed templated helices can be contrasted to weakly stabilized helices that appear within a short, simple polypeptide chain. The latter are expected to be frayed bidirectionally, resulting in an unavoidable uncertainty in defining the helical locus. Near the template–helix junction and extending some direction from it, a templated helix can be characterized both conformationally and spectroscopically. As models for studying the intrinsic properties of helices in solution, templated helices thus offer two potential advantages over short natural peptides with demonstrable helicity—conformational characterizability and a built-in reporter function.

Model Systems

Two series of peptide conjugates of 1 (X = peptide) are examined in this paper, simple alanine oligomers Ac-Hel_1-(L-Ala)$_n$-OtBu where n = 1–6 and alanine oligomers in which the template-bridging amino acid is sarcosine (N-methylglycine), Ac-Hel_1-Sar-(L-Ala)$_n$-OtBu where n = 1–4. Derivatives were prepared from the monoamino acid conjugates Ac-Hel_1-Xxx-OH, where Xxx = L-Ala or Sar, and H-L-Ala-OtBu by standard peptide coupling reactions in DMF solution using either diisopropyl carbodiimide or 1-[3-(dimethylamino)propyl]-3-ethylcarbodiimide as coupling agent and 1-hydroxybenzotriazole as a racemization

(12) Nemethy, G.; Phillips, D. C.; Leach, S. J.; Scheraga, H. A. *Nature* **1967**, *214*, 363–365.
(13) Karle, I. L.; Flippen-Anderson, J.; Sukumar, M.; Balaram, P. *Proc. Nat. Acad. Sci. U.S.A.* **1987**, *84*, 5087–5091. Bosch, R.; Jung, G.; Schmitt, H.; Winter, W. *Biopolymers* **1985**, *24*, 979–999.
(14) Karle, I. L.; Flippen-Anderson, J. L.; Uma, K.; Balaram, P. *Peptides, Chemistry, Structure, and Biology*; Rivier, J. E., Marshall, G. R., Eds.; ESCOM: Leiden, 1990; pp 544–547.
(15) Karle, I. L.; Flippen-Anderson, J. L.; Sukumar, M.; Balaram, P. *Int. J. Peptide Protein Res.* **1988**, *31*, 567–576.
(16) Marshall, G. R.; Beusen, D. D.; Clark, J. D.; Hodgkin, E. E.; Zabrocki, J.; Leplawy, M. T. *Peptides, Chemistry, Structure, and Biology*; Rivier, J. E., Marshall, G. R., Eds.; ESCOM: Leiden, 1990; pp 873–876.

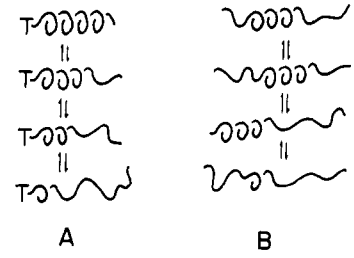

Figure 2. (A) Helical conformational states of a template-nucleated helix fray only from the distal end. (B) Peptide-nucleated helical conformations can fray from either end.

Table I. Demonstration of Peptide Fraying as a Function of *s* Value[a]

A. Fractional Population of Helical States for a Templated Hexapeptide

	% of overall population			
state	*s* value = 3.0	1.6	1.0	0.7
c-c-c-c-c-c	0.1	2.3	14.3	32.7
h-c-c-c-c-c	0.3	3.7	14.3	22.9
h-h-c-c-c-c	0.8	5.9	14.3	16.0
h-h-h-c-c-c	2.5	9.5	14.3	11.2
h-h-h-h-c-c	7.4	15.2	14.3	7.9
h-h-h-h-h-c	22.2	24.4	14.3	5.5
h-h-h-h-h-h	66.7	38.9	14.3	3.8

B. Fractional Coil Character at Each Residue Site of a Templated Hexapeptide

	residue site (%)					
s	1	2	3	4	5	6
3.0	0.1	0.4	1.2	3.7	11.1	33.3
1.6	2.3	6.0	12.0	21.4	36.4	60.5
1.0	14.3	28.6	42.9	57.2	71.5	85.8
0.7	32.7	55.6	71.5	82.8	90.7	96.2

[a] Values calculated from eq 4 of the Appendix, with all $K_i = s$.

suppressant. Alternatively, derivatives were prepared by template acylation of peptides preformed by solid-phase synthesis and were purified by flash chromatography or preparative HPLC and characterized by mass spectrometry and high-field ^{1}H NMR. The Ala and Sar monoamino acid conjugates were prepared from H-Xxx-OtBu and 1 (X = OH) by analogous couplings in yields of 80% and 60%, respectively. Synthesis and study of selectively deuterated Ala oligomers were carried out to permit unique NMR assignments of NH resonances.

All NMR studies were facilitated by the relatively high solubility of the template–peptide conjugates, which greatly exceeds those of the peptides themselves. The unusual water solubility of Ac-Hel$_1$-OH noted in the accompanying paper thus finds a parallel in the properties of its peptide conjugates. Selected derivatives were checked in each solvent for concentration dependences of δ values, which would suggest molecular association. Thus in CD_3CN a variation in concentration from 20 to 1 mM resulted in no significant chemical shift changes. Only Ac-Hel$_1$-(L-Ala)$_6$-OtBu in $CDCl_3$ showed evidence at high concentration of association.

Effect of Solvent and Linked Peptide Residues on the Structure of the Template 1 (X = Peptide)

A. Robust Helices in Weakly Polar Solvents. Chloroform is a solvent of weak polarity that is expected to result in large *s* values and robust helix formation for alanine. In it NMR spectra of the series Ac-Hel$_1$-(L-Ala)$_n$-OtBu, (n = 1–6) show a striking correlation of peptide chain length with the C-12 resonances areas assigned to (t) and (c) states. In $CDCl_3$ the monoalanine derivative shows doubling of C-12 resonances at δ 3.95 (t) and 3.82 (c) in an area ratio of 1:3, with a corresponding doubling of other peaks. For the dialanine derivative, the ratio is 4:1, and for all other oligomers, only the (t) resonance at δ 4.00 is observed. As noted in Table II, similar behavior is observed in another weakly basic solvent CD_3CN.

Table II. Dependence of Template s-cis/s-trans Ratio on Solvent and Peptide Length *n* for Ac-Hel$_1$-(L-Ala)$_n$-OtBu

solvent	*n*	trans/cis[a]
$CDCl_3$	1	0.50
	2	4.0
	3–5	>97
CD_3CN	1	2.0
	2	20
	3–5	>97
DMF-d_7	1	0.32
	2	1.9
	3	1.5
	4	3.8
	5	5.3
	6	6.7
DMSO-d_6	1	0.35
	2	0.49
	3	0.54
	4	0.61
	5	0.67
	6	0.61

[a] Obtained as the area ratio for the (t) and (c) C-12 proton resonances.

As depicted in Figure 3a the length-dependent increase in the acetamide (c)/(t) ratio in $CDCl_3$ is correlated with striking chemical shift changes of template resonances in the δ 2–3 region, assignable to the C-9 and C-13 methylene protons (the a and b proton assignments for these resonances were deduced from NOE interactions described in a subsequent section). The spectra of triAla and the higher oligomers correspond to only one slowly equilibrating species and are invariant in the template region with increasing peptide length. A 2D COSY analysis on Ac-Hel$_1$-(L-Ala)$_4$-OtBu in $CDCl_3$ generated the assignment of template resonances listed in Table III, which also includes for comparison the chemical shift values for the (cs) state of Ac-Hel$_1$-OMe in $CDCl_3$. The spectra of the mono and diAla derivatives can be described as a weighted sum of spectra of this limiting Ala$_n$ species together with that of the simple template ester.

The observed chemical shift changes are uniquely consistent with a change in conformation of the eight-membered ring from (s) to (e). From data of Table I of the accompanying manuscript, the (cs) to (ts) conversion of **1a** (X = OH) results in chemical shift changes greater than δ 0.1 only for resonances of protons at C-12, C-13a, and C-13b of pyrrolidine 1, and at C-5 of pyrrolidine 2, all neighboring the acetamido function. By contrast, 9 out of 13 template resonances for the two limiting spectra of Table III show a significant change. The shifts at C-8, C-9a, and C-9b all exceed δ 0.25 Figure 3b, and these must reflect a major change in conformation of the eight-membered ring, signaled independently by striking changes in the vicinal coupling constants $J_{H8,H9}$ at the C-8–C-9 bond. As noted in the accompanying paper, Ac-Hel$_1$-OMe is largely present as the (s) state and shows $J_{H8,H9a}$ of 9.9 Hz and $J_{H8,H9b}$ of 5.3 Hz. The corresponding values for Ac-Hel$_1$-(L-Ala)$_4$-OtBu are 5.3 and 2.5 Hz. As noted in the accompanying paper, there are two conformational energy minima for internal rotation at the C-8–C-9 bond, with a small energy barrier between them. J values of 9.9 and 2.5 Hz are close to the maximum and the minimum values

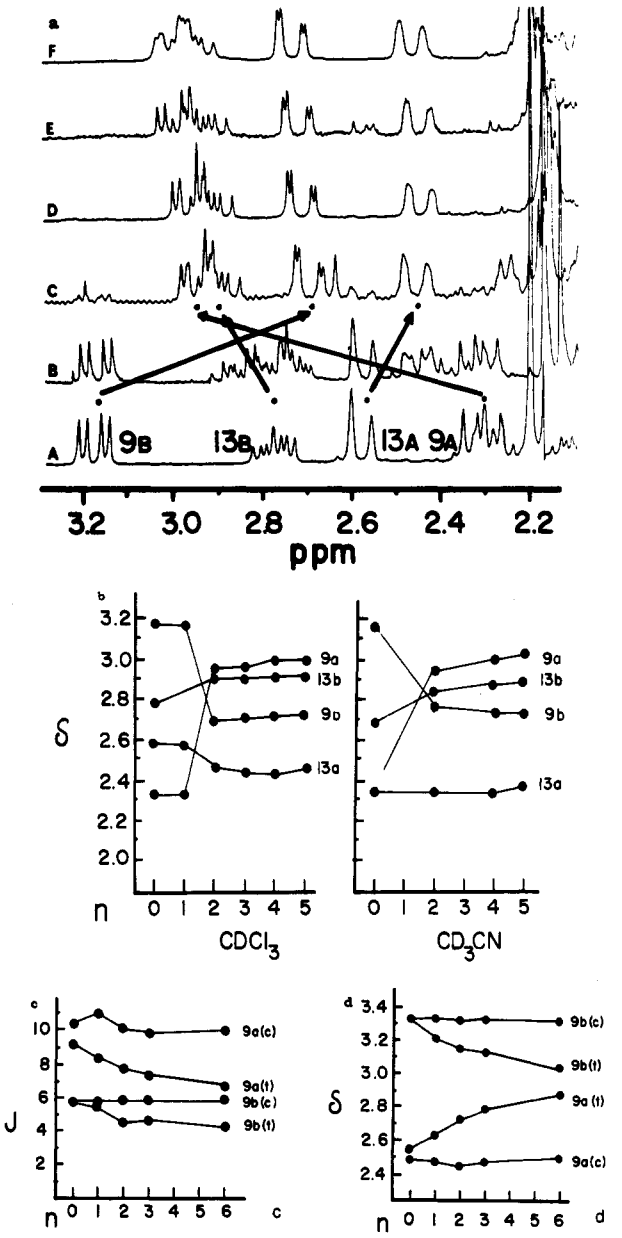

Figure 3. (a) ^{1}H NMR spectra of the C-9 and C-13 protons of Ac-Hel$_1$-(L-Ala)$_n$-OtBu conjugates in $CDCl_3$ at 23 °C as a function of chain length: A, n = 0; B, n = 1; C, n = 2; D, n = 3; E, n = 4; F, n = 5. (b) Correlation of chain length with changes of C-9 and C-13 chemical shifts for Ac-Hel$_1$-(L-Ala)$_n$-OtBu conjugates in $CDCl_3$ and CD_3CN (compare with Figure 3a) at 23 °C. (c) Correlation of chain length with changes in vicinal coupling constants $J_{8,9a}$ and $J_{8,9b}$ for Ac-Hel$_1$-(L-Ala)$_n$-OtBu conjugates in water at 23 °C. (d) Correlation of chain length with changes in C-9 proton chemical shifts for (c) (nonnucleating) and (t) (nucleating) states of Ac-Hel$_1$-(L-Ala)$_n$-OH conjugates in water at 23 °C.

expected for vicinal coupling, and it is therefore likely that the 9.9 → 5.2 and 5.3 → 2.5 Hz changes of vicinal coupling constant observed in $CDCl_3$ and in CD_3CN when a peptide is conjugated with the template are consistent with an nearly complete conformational change from an (s) to an (e) state, which reorients pyrrolidine-1 and its attached acetamido function in a geometry more appropriate for helix nucleation.

Examination of template-derived resonances for members of the series Ac-Hel$_1$-Sar-(L-Ala)$_n$-OtBu (n = 1–4) in $CDCl_3$ solution establishes the key point that the length-dependent change in conformational state of the template observed with the series Ac-Hel$_1$-(L-Ala)$_n$-OtBu is completely suppressed by the substitution of a sarcosine (*N*-methylglycine) for the first alanine residue. In the sarcosine series, peaks are doubled, owing to the presence of s-cis/s-trans isomerization at the tertiary amide bond of the sarcosine, but both coupling constants and chemical shift values for template resonances are very similar to those found for 1 = Ac-Hel$_1$-OMe, which assumes the staggered (cs) conformation in $CDCl_3$. The template is therefore locked in the nonnucleating conformation for this series of derivatives. No significant changes in δ or J values for template resonances are seen as the alanine chain length is increased, and the s-cis/s-trans ratio of the sarcosine function shows no change with increase of peptide length through the series n = 1–4. Molecular mechanics simulations of the conformation of the sarcosine derivatives at the sarcosine–template junction imply that the ψ angle that corresponds to minimum energy is ca. 160° and that the helical configuration at this site is 5 kcal/mol less stable.

In summary, NMR spectra of Ac-Hel$_1$-(L-Ala)$_n$-OtBu conjugates in $CDCl_3$ and CD_3CN show an abrupt, large increase in (t)/(c) with increase in n, and this change is correlated with changes in template δ and J values, signaling complete conversion to the template (te) state. In these solvents, the conjugates behave as robust helices, for which a single conformational mismatch at the template-helix junction is sufficient to destroy nucleation.

B. Frayed Helices in Hydrogen Bonding Solvents. DMF-d_7 has basic carbonyl lone pairs that can compete with peptide carbonyls in forming hydrogen bonds. In such a solvent the s value is expected to be small, and helices should be frayed structures. The data of Table II and Figure 4 indicate that the template (c)–(t) conversion is incomplete in this solvent, and a progressive stabilization of the (t) template conformer is observed with increasing length of peptide. A length dependence similar to that shown for DMF is obseved in water.[10]

DMSO-d_6 is an aggressively hydrogen bond forming solvent that is known from studies with polymers to strongly inhibit helix formation.[6] In this solvent, only a modest length-dependent change in the template (c)/(t) ratio is observed.

From the analysis of Figure 1, in solvents for which s is small, one expects a monotonic, convergent change with length of the (ts) to (te) state weighting for (t)-state template δ and J values. Interference of the solvent methyl peaks obscures the interpretation of the DMF-d_7 spectrum, and the instability of helical conformers of any length in DMSO-d_6 makes this solvent unsuitable for a detailed analysis of this kind. However, clear-cut data are available for a third hydrogen-bonding solvent, water, for which (c)- and (t)-state δ and J values for the template C-9 resonances are included in Table IIIb and Figure 3cd. (More detailed results for water, including results of NOE experiments are reported elsewhere.)[10]

As expected, the data obtained in water for the nonnucleating (c) states show no detectable length dependence. For the (t) states, both the vicinal $J_{8,9a}$ values and the 9a and 9b δ values show a convergent rather than an abrupt length dependence. However, the limiting $J_{8,9a}$ value is ca. 6 Hz, which is in reasonable agreement with the value of 5.9 Hz found in DMSO-d_6 and less than the values of 5.1 and 5.3 Hz found, respectively, in $CDCl_3$ and CD_3CN. These results are consistent with the presence of a significant fraction of nonhelical (ts) character in the (t) state conformational average.

As noted above, Ac-Hel$_1$-(L-Ala)$_n$-OtBu oligomers in weakly polar organic solvents undergo a simultaneous

Table III. Peptide-Induced Template Conformational Changes

A. 2D COSY Analysis of Ac-Hel$_1$-OMe and AC-Hel$_1$-(L-Ala)$_4$-OtBu in $CDCl_3$

proton	cross-peaks	Ac-Hel$_1$-OMe	Ac-Hel$_1$-(L-Ala)$_4$-OtBu δ	$\Delta\delta$
2	13ab	4.67	4.50	−0.17
5	6ab	4.65	4.54	−0.11
8	9ab, 7a	4.38	4.12	−0.26
12	11, 13a	3.83	3.94	0.11
11	12, 13ab	3.61	3.64	0.03
9b	8, 9a	3.18	2.65[a]	−0.53
13b	2, 11, 13a	2.78	2.86	0.08
13a	2, 12, 13b	2.58	2.37[a]	−0.21
9a	8, 9b	2.32	2.92[a]	0.60
7a	6a, 7b, 8	2.30	2.09	−0.11
Ac		2.20	2.20	
6b	5,7b	2.11	ca. 2.1	
6a	5, 6b, 7a	1.96	ca. 2.1	
7b	7a, 6b	1.76	ca. 1.9	0.1

B. Chemical Shifts and Vicinal $J_{8,9a}$ Values for Ac-Hel$_1$-(L-Ala)$_n$-X as a Function of Solvent and Chain Length n

solvent	n	c/t[b]	δ_{9a}	$\Delta\delta$[c]	$J_{8,9a}$ (Hz)	δ9b	$\Delta\delta$[d]	$J_{8,9b}$ (Hz)
$CDCl_3$	0	c	2.32		9.9	3.18		5.3
X = OtBu	1	c	2.32	0.00	9.9	3.17	−0.01	5.3
	2	c	2.32	0.00	9.2	3.17	−0.01	5.5
	1	t	2.46	0.14	1.5	2.86	−0.32	4.4
	2	t	2.95	0.63	4.5	2.70	−0.48	2.3
	3	t	2.96	0.64	5.0	2.72	−0.46	2.5
	4	t	3.00	0.68	5.2	2.73	−0.45	2.5
	5	t	3.00	0.68	5.1	2.74	−0.44	2.3
CD_3CN	0	c	2.23		10.0	3.05		5.6
X = OtBu	1	c	*d*	*d*	*d*	3.17	0.12	5.4
	2	c	*d*	*d*	*d*	3.18	0.13	5.5
	0	t	2.22	−0.01	9.0	3.10	0.05	5.4
	1	t	2.85	0.63	3.7	2.82	−0.28	5.4
	2	t	2.95	0.72	5.4	2.78	−0.27	3.1
	4	t	3.03	0.80	5.4	2.75	−0.30	3.0
	5	t	3.06	0.83	5.3	2.75	−0.30	2.6
DMSO-d_6	0	c	2.47		9.8	3.18		5.4
X = OtBu	2	c	2.45	−0.02	9.8	3.17	−0.01	5.5
	3	c	*d*	*d*	c	3.17	−0.01	5.0
	4	c	*d*	*d*	c	3.17	−0.01	5.5
	5	c	2.43	−0.04	9.7	3.17	−0.01	5.6
	0	t	2.42	*d*	9.3	*d*	*d*	*d*
	2	t	2.84	0.42	5.4	2.98	−0.20	3.8
	3	t	2.85	0.43	5.7	2.97	−0.21	3.7
	4	t	2.86	0.44	6.2	2.98	−0.20	3.8
	5	t	2.87	0.45	5.9	2.98	−0.20	3.8
D_2O	0	c	2.50		10.3	3.32		*d*
X = OH	1	c	2.48	−0.02	11	3.33	−0.01	5.9
	2	c	2.45	−0.05	10	3.32	0.00	5.9
	3	c	2.48	−0.02	9.8	3.33	0.01	5.9
	6	c	2.50	0.00	10	3.31	−0.01	6.0
	0	t	2.56	0.06	9.1	3.34	0.02	5.9
	1	t	2.64	0.14	8.4	3.20	−0.12	5.6
	2	t	2.74	0.24	7.7	3.15	−0.17	4.5
	3	t	2.80	0.30	7.4	3.13	−0.19	4.7
	6	t	2.88	0.38	6.6	3.04	−0.28	4.3

[a] Peaks were assigned using ROESY data as described in the NOE section of the text. [b] c = cis, t = trans conformer. [c] $\Delta\delta = (\delta_{peptide} - \delta_{Ac\text{-}Hell\text{-}OMe}(c))$. [d] Resonance cannot be assigned owing to peak overlap.

two-element conformational change from a (cs) to a (t) state that is dominated by (te) character. In hydrogen-bonding solvents, a three-state model must be used in which a nonhelical (cs) state is in slow equilibrium with a rapidly equilibrating mixture of nonnucleating (ts) state and a succession of helical (te) states. The results from four aprotic solvents and for water are thus consistent with helical nucleation by the template, but with different, solvent-dependent efficiencies of helical propagation. Spectra of the Ac-Hel$_1$-(L-Ala)$_n$-OtBu series show that elongation at the peptide chain terminus has a readily demonstrable conformational effect that is transmitted to the template acetamide function at the opposite end of the molecule. This transmission is destroyed by one disruptive element at the template–peptide junction. The overall conjugate thus behaves as a conformationally responsive whole, with structural changes at any site of the molecule reflected in changes of structure at the helix terminus. The system therefore demonstrates end-to-end communication.

Evidence for Peptide Helicity

In order to establish that true helices are in fact present in (te) states of template-linked peptides, it is necessary to examine features of the ^1H NMR resonances of the peptide itself. Four types of NMR-based signatures are expected for peptides in helical conformations in organic solvents—$J_{C\alpha H\text{-}NH}$ values consistent with helical ϕ values,

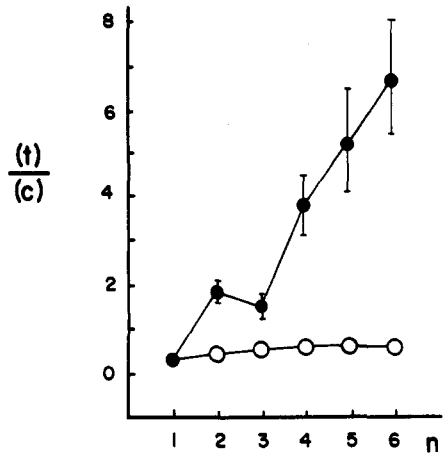

Figure 4. Variation of template (t)/(c) ratio at 23 °C for Ac-Hel_1-(L-Ala)$_n$-OtBu conjugates in DMF-d_7 (closed circles) and DMSO-d_6 (open circles) as a function of chain length, n. Error bars were calculated for a 2% error in the integrated area of the smaller peak.

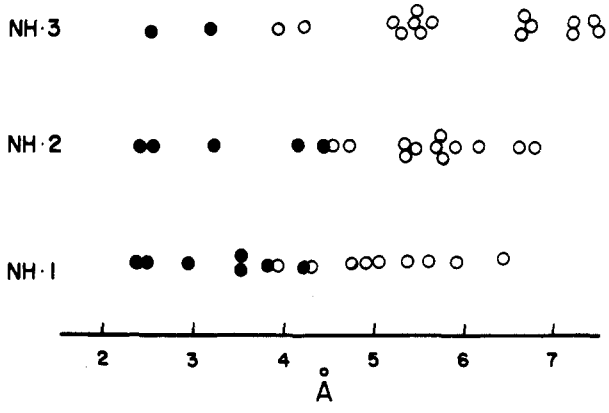

Figure 5. Results of 1-D NOE experiments on Ac-Hel_1-(L-Ala)$_3$-OtBu in $CDCl_3$. The three NH resonances were irradiated sequentially. Circles correspond to distances from each alanine NH to every template proton for the helical energy minimum calculated by molecular mechanics for Ac-Hel_1-(L-Ala)$_3$-NH-Me. Solid circles correspond to detectable NOE interactions; open circles imply no detectable NOE interaction.

$\Delta\delta/\Delta T$, and $\Delta\delta/\Delta$(solvent) values for NH resonances that are consistent with shielding from solvation of internally hydrogen bonded amides and NOE effects consistent with helical structure.[17] Peptide–template conjugates were studied in the four organic solvents, $CDCl_3$, CD_3CN, DMF-d_7, and DMSO-d_6. The NH resonances for members of the templated Ala oligomer series have been assigned to specific amino acid residues by preparation and study of deuterium-labeled analogues.

In all experiments the separation of template resonances into two conformational populations corresponding to (c) and (t) amides was mirrored quantitatively in an analogous separation of the peptide NH resonances, although in the most highly nucleating solvents $CDCl_3$ and CD_3CN, amide resonances corresponding to the nonnucleated (c) state could be detected only for the mono and diAla derivatives. $J_{C\alpha H,NH}$ values, δ NH values, and their temperature dependences are listed in Table IV and will be analyzed in detail in the discussion. In general, the (te) state values show a convergence to the values expected for a classical helix as the peptide length increases, while those in the sarcosine series or those belonging to (cs) states show no correlation with amino acid site or chain length.

NOE Interactions

Peptide–template conjugates were examined by both 1D and 2D NOE techniques. Results of 1D experiments are shown in Figure 5. The circles correspond to distances between each proton of the template and each of the three Ala NH protons of Ac-Hel_1-(L-Ala)$_3$-NH-Me, calculated from the local helical energy minimum obtained by a molecular mechanics simulation in vacuum. Filled circles correspond to proton–proton interactions of Ac-Hel_1-(L-Ala)$_3$-OtBu that exhibit 1D NOE in $CDCl_3$ upon sequential irradiation of the three NH resonances interactions, and open circles correspond to proton pairs for which NOE interactions were not observed. The appearance of an NOE signal is thus seen to be accurately correlated with the pairs of nonbonded atomic distances of a structure that is primarily α, with a bifurcation at the first pair of hydrogen bonds. A similar structure is shown in Figure 9b.

The results of 2D NOE experiments provide a more detailed picture of nonbonded distances in the template–peptide conjugates, allowing simultaneous examination of the template–template, template–peptide, and peptide–peptide interactions. ROESY spectra were taken on the conjugate Ac-Hel_1-(L-Ala-d_3)-(L-Ala-d_4)-(L-Ala-d_4)-L-Ala-OtBu in $CDCl_3$ at 23 °C and the conjugate Ac-Hel_1-(L-Ala-d_4)-L-Ala-(L-Ala-d_4)-OH in 3:1 DMSO-d_6/$CDCl_3$, thereby allowing examination in a relatively nonpolar solvent of a highly stabilized helix that forces the template to assume the (t) conformation, as well as a marginally stabilized helix in a strongly hydrogen-bonding solvent that allows presence of both nonnucleating (c) and nucleating (t) template conformations. The template NOE interactions of protons 9a and 9b in the former case comprise a weak signal between 9a and proton 5, a medium-intensity signal between 9a and 13a, and a strong signal between protons 9b and 7. In 3:1 DMSO-d_6/$CDCl_3$ at 5 °C ($CDCl_3$ added to suppres chemical exchange cross peaks) the 9ab resonances for the (t) state appear as an unresolved multiplet that shows NOE interactions only with 13a, 5, and 6 or 7; by contrast, the (c) state shows interactions between 9b and 11, 9b and 12, 9b and 7, 9a and 5, and 9a and 6 or 7. These interactions provide strong independent evidence that the (c) tertiary amide state of template–peptide conjugates is associated with the (s) conformation of the lactam, and the (t) amide state, largely with the (e) state, as seen in **1ab**. Strikingly, this correlation is sustained even for a tripeptide conjugate and in DMSO, a solvent that is helix destabilizing.

Wuethrich has summarized for the commonly encountered conformations of polypeptides the distance correlations of characteristic NOE signatures.[17] Peptides in random or extended conformations are expected to show strong interactions between α-CH and consecutive NH resonances, corresponding to an average separation $d_{\alpha N}(i, i+1)$ of ca. 2.2 Å. This separation is expected to increase to 3.6 Å as a result of helix formation. Both α and 3_{10} helices are characterized by adjacent NH–NH separations $d_{NN}(i, i+1)$ of 2.8–3.0 Å, and the relative intensities of $d_{\alpha N}(i, i+1)$ and $d_{NN}(i, i+1)$ NOE signals at an amino acid locus have been used to estimate the approximate abundances of extended and helical conformations at that site. A classical α-helix is characterized by a separation of ca. 3.5 Å for $d_{\alpha N}$ $(i, i+3)$ as well as the following distances in the 3.0 Å range: $d_{NN}(i, i+1)$, $d_{\beta N}(i, i+1)$, $d_{\alpha\beta}(i, i+3)$. An α-helix is spectroscopically well-defined if NOE

(17) Wuethrich, K.; Billeter, M.; Braun, W. *J. Mol. Biol.* **1984**, 715–740. Dyson, H. J.; Rance, M.; Houghten, R. A.; Wright, P. E.; Lerner, R. A. *J. Mol. Biol.* **1988**, *201*, 210–217.

Table IV. $J_{C_\alpha H NH}$ Values, δ_{NH} Values, and $\Delta\delta/\Delta T$ Values for Ac-Hel$_1$-(L-Ala)$_n$-OtBu in Organic Solvents

A. Vicinal Coupling Constants $J_{C_\alpha H-NH}$ (Hz) for the (t) State

oligomer N =	solvent	Amino Acid Position 1	2	3	4	5	6
1	$CDCl_3$	6.8					
2		8.8	7.6				
3		8.1	8.0	7.5			
4		6.8	6.4	7.0	7.6		
5		7.0	5.3	6.6	6.2	7.6	
6		6.8	4.6	4.8	*a*	*a*	7.2
1	CD_3CN	7.5					
2		8.7	6.8				
3		8.2	8.0	7.5			
4		6.6	5.6	7.0	7.6		
5		7.4	5.0	5.3	6.2	7.6	
6		7.3	<5.0	<5.0	5.5	7.9	6.8
1	DMF-d_6	7.2					
2		8.7	7.1				
3		7.9	8.0	6.9			
4		7.3	6.2	7.4	6.7		
5		7.1	5.9	6.3	8.0	7.1	
6		7.1	5.6	5.6	7.1	8.2	7.0
1	DMSO-d_6	7.5					
2		8.4	6.9				
3		8.9	8.2	6.9			
4		7.5	7.0	7.6	7.2		
5		6.9	6.9	7.6	7.7	6.9	
6		7.8	6.3	6.8	7.6	7.6	7.9

B. δ NH Values and $\Delta\delta/\Delta T$ Values for (c) and (t) States

n position	solvent	(c/t)	δ NH value in ppm ($\Delta\delta/\Delta T$ in 10^3 ppm/K) 1	2	3	4	5	6
1	$CDCl_3$	c	6.35 (−0.1)					
		t	7.50 (−2.0)					
2		c	6.41 (−1.4)	6.40 (−1.4)				
		t	7.45 (−2.0)	7.10 (−2.6)				
3		t	7.41 (−1.9)	7.17 (−2.2)	6.94 (−2.2)			
4		t	7.36 *b*	7.15 *b*	6.94 *b*	6.93		
5		t	7.36 (−4.9)	7.33 (−2.5)	7.09 (−1.3)	7.07 (−2.4)	7.05 (−2.7)	
6		t	7.24 (0.4)	7.34 (−1.9)	7.26 (−3.2)	7.13 (−1.5)	7.13 (−1.5)	7.10 (−2.9)
1	CD_3CN	c	6.75 (−1.7)					
		t	7.37 (−2.9)					
2		t	7.34 (−1.5)	7.15 (−2.1)				
3		t	7.30 (−1.4)	7.26 (−1.7)	6.98 (−1.5)			
4		t	7.26 (−0.6)	7.40 (−2.4)	7.07 (−1.4)	6.98 (−2.1)		
5		t	7.06 (−1.2)	7.58 (−3.0)	7.35 (−3.6)	7.09 (−1.1)	7.05 (−1.7)	
6		t	6.96 (1.8)	7.61 (−2.2)	7.63 (−4.2)	7.27 (−2.2)	7.17 (−1.6)	7.13 (−2.5)
1	DMF-d_7	c	8.24 (−3.8)					
		t	7.68 (−7.7)					
2		c	7.90 (−6.6)	7.85 (−6.8)				
		t	7.52 (−2.0)	7.39 (−2.7)				
3		c	*a*	*a*	7.79 (−5.1)			
		t	7.41 (−2.5)	7.49 (−2.2)	7.50 (−3.9)			
4		c	8.21 (−7.1)	*a*	*a*	7.87 (−4.7)		
		t	7.50 (−1.9)	7.52 (−2.9)	7.40 (−2.9)	7.66 (−5.0)		
5		c	8.31 (−6.9)	7.99 (−5.9)	7.98 (−4.9)	7.97 (−6.1)	7.79 (−4.4)	
		t	7.46 (−2.8)	7.69 (−4.3)	7.65 (−3.3)	7.55 (−3.8)	7.41 (−1.3)	
6		t	7.33 (−0.7)	7.69 (−3.3)	7.68 (−4.3)	7.49 (−2.7)	7.46 (−1.4)	7.62 (−2.5)
1	DMSO-d_6	c	8.23 (−4.3)					
		t	7.69 (−2.8)					
2		c	8.13 (−6.2)	8.11 (−6.3)				
		t	7.49 (−3.1)	7.48 (−4.3)				
3		c	8.18 (−5.7)	8.12 (−4.2)	7.82 (−5.9)			
		t	7.50 (03.2)	7.39 (−3.4)	7.78 (−6.4)			
4		c	8.16 (−4.7)	8.15 (−6.1)	7.91)−5.3)	7.85 (−4.5)		
		t	7.50 (−3.4)	7.43 (−2.8)	7.60 (−5.7)	7.98 (−4.5)		
5		c	8.15 (−4.4)	8.15 (−6.1)	7.92 (−3.7)	7.89 (−5.0)	7.88 (−5.6)	
		t	7.45 (−3.2)	7.46 (−2.7)	7.62 (−4.6)	7.72 (−5.7)	8.04 (−6.4)	
6		c	8.18 (−4.7)	7.88 (−5.0)	7.87 (−5.0)	7.87 (−5.0)	7.94 *a*	8.17 (−5.0)
		t	7.44 (−2.3)	7.47 (−1.9)	7.65 (−4.3)	7.72 (−3.7)	7.76 (−4.7)	8.05 (−5.0)

[a] Assignment uncertain due to peak overlap. [b] Value not measured.

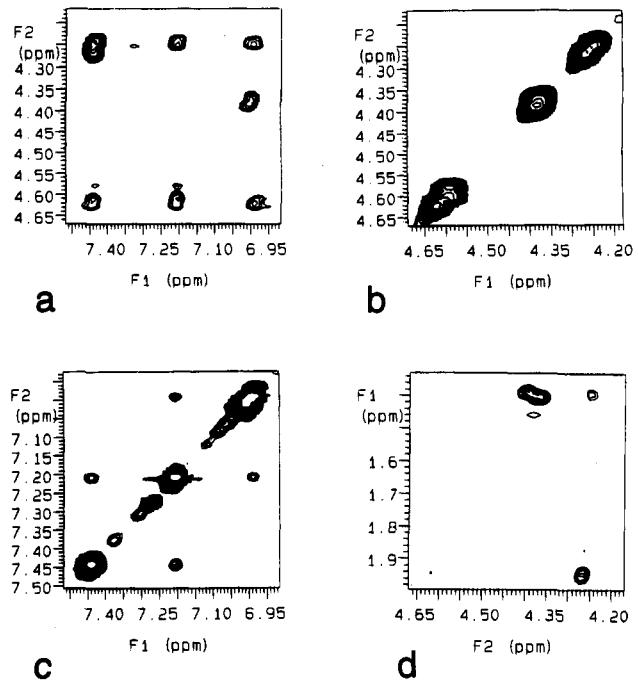

Figure 6. Selected areas of the 500-MHz ^1H phase-sensitive ROESY spectrum of Ac-Hel$_1$-(L-Ala-d_3)-(L-Ala-d_4)-(L-Ala-d_4)-L-Ala-OtBu in $CDCl_3$. (a) Spectrum portion showing the cross peaks between C-2H, C-5H, αC-H, and the NH resonances. (b) Spectrum portion showing the diagonal C-2, C-5, and α-CH peaks for reference. (c) Spectrum portion showing the NH–NH cross peaks. (d) Spectrum portion showing the cross-peaks between αC-H and βC-H.

interactions are observed for most or all of these. A 3_{10} helix is distinguished from an α by the following distances: $d_{\alpha N}(i, i+3)$ of 4.0 vs 3.6 Å, $d_{\alpha N}(i, i+2)$ of 3.5 vs 4.6 Å, and $d_{\alpha\beta}(i, i+3)$ of 5.0 vs 3.0 Å. For a 3_{10} helix the third NOE is expected to be unobservabled and the first, greatly reduced in intensity. The second should be observed only for a 3_{10} helix. The 3_{10} helix is also expected to show a distinctive series of weak to medium NOE interactions corresponding to a $d_{\alpha\beta}(i, i+2)$ of 3.6 Å.

As evidenced by the contour plots of Figure 6a–d, the ROESY spectrum of the template–tetrapeptide conjugate Ac-Hel$_1$-(L-Ala-d_3)-(L-Ala-d_4)-(L-Ala-d_4)-L-Ala-OtBu in $CDCl_3$ is characterized by the following sequential NOE interactions (relative peak heights are indicated in parentheses). Type $\alpha N(i, i+1)$: αN(C-5, NH-1) (m), αN(1, 2) (s). Type $NN(i, i+1)$: NN(1, 2) (m), NN(2, 3) (m). Type $\alpha N(i, i+3)$: αN(C-2, NH-2) (m), αN(C-5, NH-3) (s), αN(1, 4) (w). Type $\alpha\beta(i, i+3)$: $\alpha\beta$(1, 4) (m). Type $\alpha N(i, i+2)$: αN(C-2, NH-1) (w), αN(C-5, NH-2) (m), αN(1, 3) (ms). An additional medium-intensity helical peptide–template interaction between NH-1 and the proton at C-8 is observed, and of the nine expected interactions characteristic of an α-helix, only the $\beta N(i, i+1)$ (C-6, NH-1) and $\alpha N(i, i+3)$ (acetyl, NH-1) NOEs are ambiguous, owing to overlap of Ac, C-7, and C-6 resonances. (The $NN(i, i+1)$ interaction expected between NH-3 and NH-4 is not observed owing to peak overlap.) The medium-intensity $\alpha\beta(i, i+3)$ interaction establishes the helix unambiguously as having α-character; however, the observation of all $\alpha N(i, i+2)$ interactions expected for a 3_{10} helix implies that the actual helix in this nonbasic solvent is best described either as an α-3_{10} hybrid with an extensive series of bifurcated hydrogen bonds or as a rapidly equilibrating ensemble of the two structures.

The ROESY spectrum of the template–tripeptide conjugate Ac-Hel$_1$-(L-Ala-d_4)-L-Ala-(L-Ala-d_4)-OH in 3:1 DMSO-d_6/$CDCl_3$ allows examination of both nucleated (te) and nonnucleated (cs) conformations in the same solution. The (cs) state spectrum is characterized by the following NOE interactions. Type $\alpha N(i, i+1)$: αN(C-5, NH-1 (vs), αN(2, 3) (vs). Type $\beta N(i, i+1)$: βN(C-6, NH-1) (w), βN(2, 3) (m). Type $NN(i, i+1)$: NN(1, 2) (m), NN(2, 3) (w). In addition, a weak interaction between protons on C-7 and NH-2 is observed, but strikingly, no NOE interactions extending beyond four bonds and involving the peptide hydrogens can be observed for the (cs) conformational manifold. We interpret the observed medium and weak $NN(i, i+1)$ interactions as signifying the presence of a moderately stable type 1 β-turn structure in equilibrium with more abundant extended peptide conformations.[18]

The (te)-state spectrum is characterized by the following NOE interactions. Type $\alpha N(i, i+1)$: αN(C-5, NH-1) (s), αN(2, 3) (s). Type $\beta N(i, i+1)$: βN(C-6, NH-1) (w), βN(2, 3) (w). Type $NN(i, i+1)$: NN(1, 2) (s), NN(2, 3) (m). Type $\alpha N(i, i+3)$: αN(C-5, NH-3) (w). Type $\alpha\beta(i, i+3)$: $\alpha\beta$(C-2, 2-βCH_3) (w). Owing to a coincidence of resonances for C-2 and C-5 protons, a medium-intensity cross-peak between this composite resonance and NH-2 cannot be assigned unambiguously either to an $\alpha N(i, i+3)$ or to an $\alpha N(i, i+2)$ interaction. Similarly, a possible $\alpha N(i, i+2)$ interaction between C-2 and NH-1 cannot be assigned in the presence of the strong $\alpha N(i, i+1)$ cross-peak between C-5 and NH-1. A cross-peak corresponding to the $\alpha N(i, i+3)$ interaction between the acetyl and NH-1 is not observed. With this exception, all of the expected peaks for a helical structure are found in this ROESY spectrum; unfortunately, owing to the C-2, C-5 peak coincidence, the importance of 3_{10} structures for helical states in this aggressively hydrogen-bonding solvent cannot be assessed.

Length and Solvent Dependencies of Peptide NMR Parameters

All ^1H NMR parameters, such as NOE data, vicinal CαH–NH coupling constants, δ_{NH} values, and their temperature and solvent dependences, are energy-weighted averages of values for accessible conformations of a peptide backbone, and this point has been carefully demonstrated for cyclic peptides.[18-20] If the model of Figure 1 is correct, all (c)-state peptide resonances of Ac-Hel$_1$-(L-Ala)$_n$-X as well as all conformations of the sarcosine derivatives are expected to exhibit parameters indistinguishable from those of the random coil. The (t)-state peptide resonances observed in solvents that support robust helices are expected to be those of the all helical state. By contrast, (t)-state resonances observed in solvents that support frayed helices are averaged in two ways: first, through inclusion of the nonhelical (ts) state in the state sum, and second, through averaging through the series of (te) states. The amino acid residues of a helix that is progressively frayed distal to the template region thus will exhibit (t)-state NMR signatures that converge to those expected for the random coil as distance of the amino acid residue from the template is increased. This effect is expected to be moderate in DMF and most significant in the structure-breaking solvent DMSO, which should show a readily

(18) Venkatachalapathi, Y. V.; Venkataram Prasad, B. V.; Balaran, P. *Biochem.* **1982**, *21*, 5502–5509.
(19) Gierasch, L. M.; Deber, C. M.; Madison, V.; Niu, C.-H.; Blout, E. R. *Biochemistry* **1981**, *20*, 4730. Rose, G. D.; Gierasch, L. M.; Rockwell, A. L.; Thompson, K. F.; Briggs, M. S. *Biopolymers* **1985**, *24*, 117. Kessler, H. *Angew. Chem., Int. Ed. Engl.* **1982**, *21*, 512–523.
(20) Pitner, T. P.; Urry, D. W. *J. Am. Chem. Soc.* **1982**, *94*, 1399. Kessler, H.; Hehlien, W.; Schieck, R. *Ibid.* **1982**, *104*, 4534.

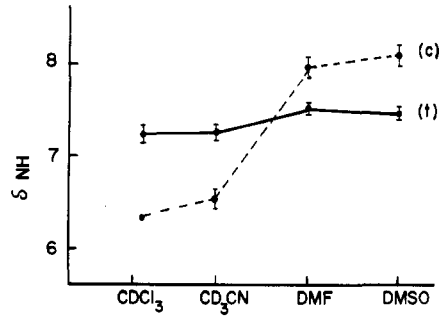

Figure 7. Mean and standard deviations of the chemical shifts of ^{1}H NMR resonances of (c) and (t) states for the peptide NHs of Ac-Hel$_1$-(L-Ala)$_n$-OtBu conjugates in four solvents at 23 °C. Only data for residues 2–4 are averaged for the DMSO (t) states.

apparent position-dependent convergence of δ and J to random coil values as one progresses from the proximal to the distal end of the peptide.

For NH protons, shielding from interactions with solvent, whether through hydrogen bonding or steric inaccessibility, is usually deduced from the solvent and temperature dependences of the NH chemical shifts.[19,20] Figure 7 shows the mean and standard deviation of the alanine NH values for all Ac-Hel$_1$-(L-Ala)$_n$-OtBu oligomers for which both (c) and (t) states can be detected. (The DMSO (t) states are represented only by data for the first two alanine residues.) The δ values for the (t) states are only modestly dependent on solvent, as expected for resonances corresponding to internally hydrogen bonded protons, but the δ values for the (c) states show the full variation that has been observed in other studies for solvent-exposed NH protons. Solvent dependences thus support the structural assignment of helical (t) and random coil (c) states.

For the (t)-state resonances of a conjugate in a structure-breaking solvent, as distance of an NH from the template is increased, convergence of peptide δ NH to a random coil value is expected. From the data of Table IV this feature is readily seen for the penta and hexa-Ala conjugates in DMSO. Whereas the (c) states of the Ala conjugates show an average δNH of δ 7.99 (standard deviation = 0.15), with a correlation coefficient (C.C.) of only 0.31 between the amino acid rank and the δ NH value, the (t) states show a C.C. of 0.95 between rank and δ, with a mean of δ 7.68 (0.23). The average for δ NH values of residues 5 and 6 is δ 7.91, indistinguishable from the mean of the (c) values. Correlations between (t)-state rank and δ NH are not usual for the other solvents in the study (for MeCN: C.C. = −0.16; for DMF: C.C. = 0.21). The structure-breaking feature of DMSO is thus directly reflected in a rapid convergence of δ NH values to those expected for a random coil as the sequence separation from the template is increased. As noted below, similar convergences of J values and $\Delta\delta/\Delta T$ values are also seen in this solvent, as is evident in Figure 8.

The δ values of solvent-exposed NH protons usually show a characteristic solvent-dependent negative temperature coefficient, owing presumably to a selective decrease with increasing temperature of solvent–solute interactions.[21] The different temperature dependences of δ values for solvent shielded and exposed protons have been reported for a number of solvents, but the distinction is most reliable in basic solvents that form strong hydrogen bonds. Abundant data have been collected for DMSO-d_6, for which values of $-\Delta\delta/\Delta T \times 10^3$ ppm/K of less than 3

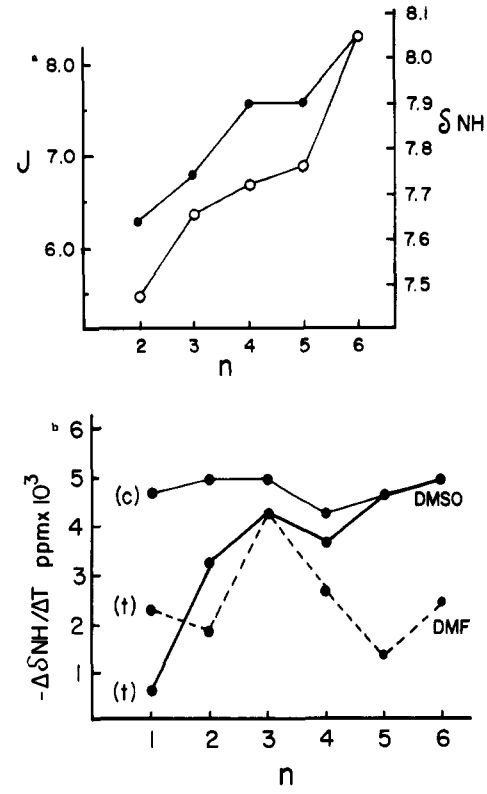

Figure 8. (a) Variation of NH chemical shift (open circles) and vicinal coupling constant $J_{C_\alpha H,NH}$ (closed circles) with amino acid position n for the conjugate Ac-Hel$_1$-(L-Ala)$_6$-OtBu in the structure-breaking solvent DMSO-d_6 at 23 °C. (b) Temperature dependence of the NH chemical shifts for the (c) and (t) states of Ac-Hel$_1$-(L-Ala)$_6$-OtBu in the structure breaking solvent DMSO-d_6 (continuous lines) and for the (t) state in DMF-d_7 (dotted line).

are usually regarded as consistent with hydrogen bonding or sequestering from solvation, while values of 5 or greater are typical of hydrogen bonding to solvent.[19] For the 20 (c)-state NH resonances observed for Ac-Hel$_1$-(L-Ala)$_n$-OtBu in DMSO-d_6, all but one lie above 4, and the mean value observed is 5.1 (0.8). The mean $-\Delta\delta/\Delta T \times 10^3$ ppm/K value for NH resonances for the sarcosine derivatives Ac-Hel$_1$-Sar-Ala$_n$-OtBu, n = 1–4, in DMSO is 5.68 (0.88). The (c) states in polar solvents are therefore characterized by solvent-exposed peptide NH groups, as seen in Figure 8b.

The 10 (t)-state NH resonances observed in DMSO for residues 1 or 2 show a $-\Delta\delta/\Delta T \times 10^3$ ppm/K range of 1.9–3.4, with a mean of 2.88 (0.49), consistent with a large degree of solvent shielding. Other residues show the length-dependent convergence to a higher value expected in this structure-breaking solvent; thus, for Ac-Hel$_1$-(L-Ala)$_6$-OtBu, residues 5 and 6 show values of 4.7 and 5.0, respectively. Figure 8b demonstrates the convergence with increasing length to solvent exposed values.

Although correlations have also been reported in the nonbasic solvent $CDCl_3$,[22] their interpretation is more problematic, and this ambiguity is likely to be shared with data from the weakly basic solvent CD_3CN. In $CDCl_3$, values close to 2.4 have been attributed to solvent-exposed amide NH protons, internally hydrogen-bonded or solvent-shielded hydrogens are reported to have values less than or equal to 2.4, and intermolecularly hydrogen bonded protons or protons in conformations that undergo detec-

(21) Llinas, M.; Klein, M. P. *J. Am. Chem. Soc.* **1975**, *16*, 4731–4737.

(22) Stevens, E. S.; Sugawara, M.; Bonora, G. M.; Toniolo, C. *J. Am. Chem. Soc.* **1980**, *102*, 7048–7050.

tible change with temperature increase show values considerably greater than 2.4.[22]

Examination of the temperature dependence data of Table IV shows that in $CDCl_3$ a majority of (t) states appear to be solvent shielded, with several noteworthy exceptions. The NH distal to the template usually shows a value higher than 2.4, suggesting conformational equilibration, the proximal NH shows an anomalous value for the longer oligomers, and NHs at sites 2 or 3 show large values, suggesting conformational inhomogeneity. A very similar pattern is seen in CD_3CN for which literature precedents are not available. It is particularly striking that the values of $-\Delta\delta/\Delta T \times 10^3$ ppm/K for Ac-Hel$_1$-(L-Ala)$_6$-OtBu in this part of solvents exhibit a C.C of 0.985, suggesting that these data are generalizable and reflect conformational attributes of the peptide itself that are likely to be assumed in all solvents of comparable polarity.

Although DMF-d_7 lacks a significant data base of literature $\Delta\delta$NH/ΔT values, this rather basic solvent supports helices and is expected to follow the simple temperature dependence patterns of DMSO and water. The mean $-\Delta\delta/\Delta T \times 10^3$ ppm/K value observed for the (c) states is 5.67 (1.14), and that observed for the sarcosine conjugates in this solvent is 5.96 (0.69), both consistent with exposure to solvent molecules. By contrast, the mean value in DMF-d_7 for the (t) states is 2.87 (1.08). For $n <$ 5 the pattern of variations of temperature dependences is unremarkable, but for the penta and hexaAla derivatives, as seen in Figure 8b, a maximum value is seen at residues 2 or 3, similar to that observed in the nonpolar solvents.

Molecular modeling provides some insight into the structural effects that may underlie these observations. The Ac-Hel$_1$-(L-Ala)$_n$-NHMe structures, n = 1–5, were placed in an α-helical (te) conformation and locally minimized in vacuum. For n = 1 and 2, the local minimum corresponds to a 3_{10} helix, with each peptide NH hydrogen bonded to a single template carbonyl (Figure 9a). In rough accord with the more detailed modeling carried out by Marshall for untemplated helices,[16] for larger peptides the α-helix becomes the more stable conformation. Thus for $n > 2$, the local minimum is a modified α-helix in which the NH of Ala-1 involved in a 3_{10}-α bifurcated hydrogen bond, as noted in Figure 9b.

From this model a transition from 3_{10} to α-structure is expected when the peptide provides four NH hydrogen bonding sites, which first occurs with Ac-Hel$_1$-(L-Ala)$_3$-NHMe for the simulation and Ac-Hel$_1$-(L-Ala)$_4$-OtBu among the experimental cases. A change of structure is expected as the chain is increased from three to four residues, and the longer structure should contain an hydrogen bond anomaly or conformational readjustment among its early residues that may be reflected in increased solvent exposure for an NH. In hydrogen bond sustaining solvents, contributing conformers may contain locally interdigitated solvent molecules similar to those observed in the solid state by Karle.[14] Such an intervention would be signaled by an increase in magnitude of $-\Delta\delta$NH/ΔT.

The most incisive structural evidence concerning the conformations of the peptide sequences of templated conjugates is provided by the vicinal coupling constants $J_{C\alpha H\text{-}NH}$, which reflect backbone torsional angles ϕ.[23] A J value in the range of 6.5–7.5 Hz is usually observed for a polypeptide in a random coil state.[17] Such a value is expected for the distal residue of a templated peptide ester Ac-Hel$_1$-Ala$_n$-OtBu, since two hydrogen bonds flanking the

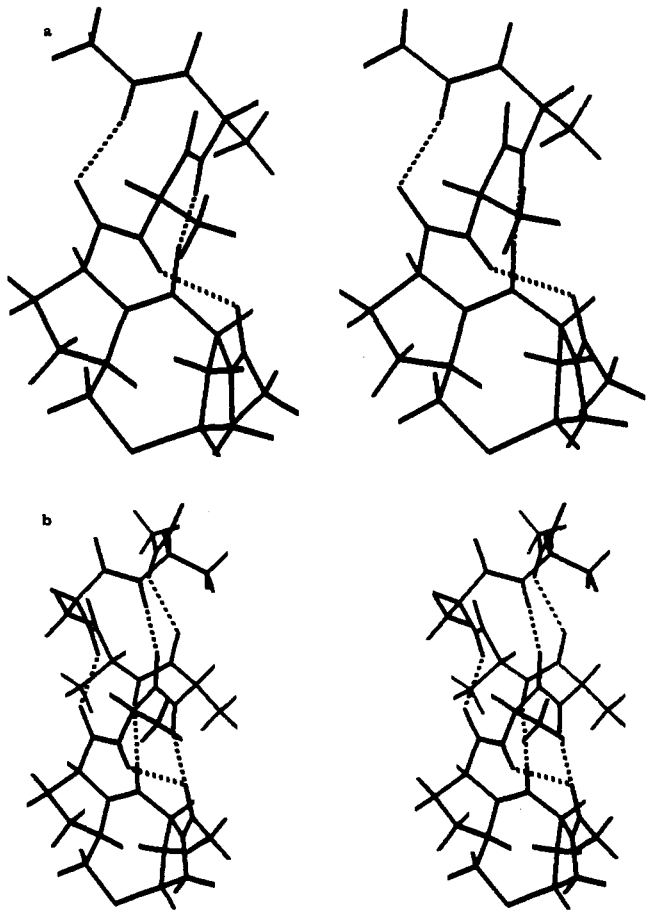

Figure 9. Computer-generated stereodiagrams of local helical minima calculated by molecular mechanics in vacuum: (a) Ac-Hel$_1$-(L-Ala)$_2$-NHMe, a (te) state of a 3_{10} helix; (b) Ac-Hel$_1$-(L-Ala)$_5$-NHMe, a (te) state of an α-helix with bifurcated H-bonds.

α-carbon of an amino acid residue are required to constrain ϕ. The mean of 20 values for the distal residue of the hexaAla conjugate in the four solvents of the study is 7.24 Hz (0.30). The mean for the alanine residues in $CDCl_3$ for the sarcosine series Ac-Hel$_1$-Sar-Ala$_n$-OtBu, (n = 1–4), for which all residues are expected to show random coil J values, is 7.31 Hz (0.33). Finally, the mean value observed for (c) states in DMSO is 7.28 Hz (0.31), and (t) states in that solvent for residues 4, 5, or 6 converge to the random coil value.

Although an idealized ϕ angle for an α-helix of −57° is expected to correspond to a $J_{C\alpha H\text{-}NH}$ value of 3–4 Hz, typical experimental values lie below 6 Hz, and a low $J_{C\alpha H\text{-}NH}$ value alone is neither a necessary nor a sufficient condition for the presence of a residue in a helix.[23] In a recent study of the distorted helix alamethicin in methanol by Campbell and co-workers,[24] many residues were found in the expected range of 4.9–5.7 Hz, but substantially higher values were observed as well. In part, this finding reflects the range of −65° ± 6° for ϕ values that are actually observed for α-helices in proteins characterized by X-ray crystallography.[25]

As noted in Table IV, in all helix-supporting solvents the nonterminal residues of peptide–template conjugates show a length dependent convergence of $J_{C\alpha H\text{-}NH}$ values to those expected for an α-helix. Figure 10 plots the mean of the $J_{C\alpha H\text{-}NH}$ values, with standard deviations, at three

(23) Pardi, A.; Billeter, M.; Wuethrich, K. *J. Mol. Biol.* **1984**, *180*, 741–751. Bystrov, V. F. *Prog. NMR Spectrosc.* **1976**, *10*, 41–81.

(24) Esposito, G.; Carver, J. A.; Boyd, J.; Campbell, I. D. *Biochemistry* **1987**, *26*, 1043–1050.

(25) Chothia, C. *Ann. Rev. Biochem.* **1984**, *53*, 537–572.

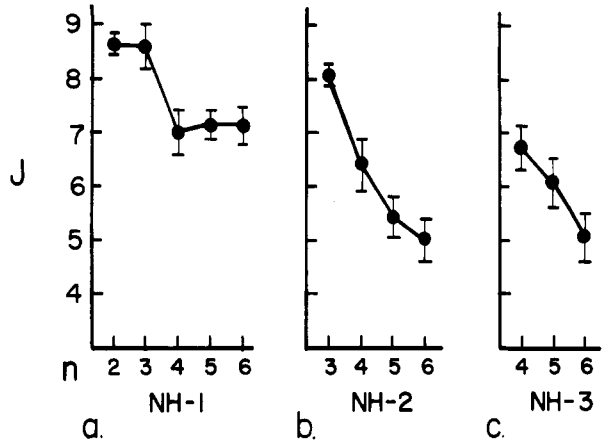

Figure 10. Vicinal coupling constants $J_{C_\alpha H,NH}$ calculated as averages of values in the four solvents, $CDCl_3$, CD_3CN, DMF-d_7, DMSO-d_6 at 23 °C for each of the conjugates Ac-Hel$_1$-(L-Ala)$_n$-OtBu (n = 2–6). Standard deviations appear as error bars; DMSO data were used for n = 2–4 only. (a) J values averaged over the four solvents for the first NH as a function of peptide length. (b) Average J values for the second NH. (c) Average J values for the third NH.

sites for the solvents of the study. The relatively small standard deviations reflects the operation of length-dependent but solvent-independent structural features of helix nucleation. Residues 2 and 3 show a strict length-dependent convergence, reaching helical $J_{C_\alpha H\text{-}NH}$ values only when five or more interior hydrogen bonds have been formed. The values for residue 1 show particularly strikingly that a length-dependent structural change occurs upon addition of the fourth Ala residue. The ROESY data reported in an earlier section establish that in chloroform the tetraAla conjugate exhibits essentially all NOE cross-peaks expected for an α-helix, but also exhibits 3_{10} character throughout its length. The large $J_{C_\alpha H\text{-}NH}$ values seen for the diAla and triAla conjugates imply that ψ for these derivatives lies in the range of −80 to −90°, consistent only with a distorted helical structure with two or three bifurcated hydrogen bonds.

For a given solvent the dependence of the (c)/(t) ratio on homopeptide length allows a calculation of the propagation parameter s for the amino acid residue in that solvent, as derived in the Appendix. Because the (c) state is undetectable for most oligomers in $CDCl_3$ and CD_3CN, the propagation parameter for alanine in these solvents can be defined only as a lower bound, which must lie in the range of 10–20. In the structure-breaking solvent DMSO the propagating factor is roughly 0.6–0.8, while in DMF, the best value appears to be 1.2–1.5. Data from larger oligomers will be required to refine the latter value, which is rendered uncertain by the local maximum exhibited by the (c)/(t) data of Table II. This maximum may reflect 3_{10}-α conformational reorganization.

The studies here reported thus lay the groundwork for an investigation in aqueous solution of the helix–coil equilibrium for short polypeptides.[10] Since the helical sequences of proteins are typically of 8–15 amino acid residues in length, the results of aqueous experiments on short peptide–template conjugates are likely to be relevant to helix formation during the folding of proteins from the denatured state. It should be noticed however that helix nucleation and formation is also observed in the highly nonaqueous environments of membrane surfaces or interiors as well as conceivably in the hydrophobic environment of molten globules. Although aqueous studies have an obvious central role in interpreting this problem, an understanding of the equilibrium aspects of helix formation will remain incomplete until results from studies in a range of organic solvents are also available.

This study has demonstrated the feasibility of both nucleation and reporting of helices by an N-terminal conformational template. How efficient is the nucleation process by Ac-Hel$_1$-X? The greater stability of the (ts) over the (te) conformation for Ac-Hel$_1$-OH in all solvents implies that as a nucleation site, this template is less than optimal. Inspection of eq 4 of the appendix reveals that an intrinsically unfavorable (ts)/(te$_1$) ratio is reflected in a small K_2 value, which in turn attenuates the influence of the geometric s series on the observed template (t)/(c) ratio, allowing a greater span of s values to fall within the range of ratios that can be measured by NMR integration. Clearly, a given template cannot be optimized for both reporter and nucleation functions, and Ac-Hel$_1$-X is in fact a nearly optimal reporter. Experiments toward redefinition of the template system to increase its nucleation capacity are in process and will be reported subsequently.

Is the template necessary for nucleation of helical structure in these solvents? A survey by Goodman and Saltman[26] of the NMR properties of linear homooligopeptides in a broad range of solvents showed disorder or irregular γ-turn like structures, except in the strongly helix-promoting solvent trifluoroethanol. We have noted that Ac-Pro-Pro-Ala$_6$-OH, a close structural analogue of Ac-Hel$_1$-Ala$_6$-OH, in water shows no evidence of helicity.[27] A conformational template is thus mandatory for helix formation in most solvents.

In this paper we have provided for the first time a detailed conformational picture of the structures of short helical polypeptide sequences in organic solvents. Complementing these results with studies of peptide conjugates with helical templates that contain a variety of different structural constraints and that nucleate from the C-terminus or from the center of helices[28] should illuminate the fundamental issues of helix formation, including the central questions of the upper bound on the nucleating efficiency of a properly optimized helical template and the roles for helix formation and stability of C- and N-terminal amino acids that may be capable of helix initiation and termination.[29]

Summary

In this study peptide conjugates of the helical template Ac-Hel$_1$-X have been shown from ^{1}H NMR evidence to assume helical conformations in the organic solvents $CDCl_3$, CD_3CN, and DMF-d_7 and for short helices in the structure-breaking solvent DMSO-d_6. The template portion of the conjugates has been shown to exist largely in two detectible conformations, a (cs) state that does not nucleate helices and a (te) state that is a potent helix nucleator. Because equilibration between these states is slow on the NMR time scale, all resonances for a peptide-template conjugate are split into pairs of integrable resonances corresponding to the slowly equilibrating (c) and (t) template states, allowing direct measurement of the ratios of these states as functions of solvent, temperature, amino acid composition, and peptide length. In addition to a nucleation function, the template thus acts as a two-state switch with a slow response time, permitting

(26) Goodman, M.; Saltman, R. P. *Biopolymers* **1981**, *20*, 1929–1957.
(27) Kemp, D. S.; Boyd, J. G. In *Peptides: Chemistry, Structure and Biology*; Rivier, J. E., Marshall, G. R., Eds.; ESCOM: Leiden, 1990; pp 677–679.
(28) Ghadiri, M. R.; Choi, D. *J. Am. Chem. Soc.* **1990**, *112*, 1630–1633.
(29) Presta, L. G.; Rose, G. D. *Science* **1988**, *240*, 1632.

for the first time direct observation and quantitation of the properties of short helices.

The peptide conformations associated with (cs) states of the template have been shown by solvent and temperature dependence of NH δ values as well as by coupling constants to be indistinguishable from random coil states. From NOE experiments in $CDCl_3$ and DMSO, peptide conformations associated with (te) states of the template exhibit the intrapeptide and interpeptide–template NOE interactions expected for template-nucleated hybrid 3_{10}-α helices. The NH protons of these conformations are solvent shielded as judged by solvent and temperature effects on δ values, and with increase of the chain length of the Ala oligomer, $J_{C_\alpha H\text{-}NH}$ vicinal coupling constants converge to α-helical values.

In a qualitative ranking of the stabilizing effects of solvents on polyglutamic acid derivatives, Fasman noted the following order of helix stabilization: $CHCl_3 \gg$ DMF $\gg$ DMSO.[6] We have confirmed this order for short helices derived from templated Ala peptides. In solvents that lack protic or basic character such as $CDCl_3$ or CD_3CN the nucleated helices are robust and show little evidence of conformational fraying. In basic aprotic solvents such as DMF or DMSO, the helices are loose and must be regarded as conformational averages of a full range of possible helical sequences, nucleated from the template region.

Experimental Section

DMF was distilled from ninhydrin and stored over sieves; it was freshly distilled before peptide coupling reactions. Diisopropylethylamine (DIEA) was distilled from ninhydrin, then from NaOH/Na, then stored over sieves. N-hydroxybenzotriazole (HOBt) 1-[3-(dimethylamino)propyl]-3-ethylcarbodiimide (EDMAPD) were used without purification.

Analytical TLC was performed on E. Merck 0.25-mm F-254 silica gel 60 plates with glass backing. Analytical HPLC was performed on a Vydac C_{18} reversed-phase column.

Preparation of Ac-Hel$_1$-L-Ala-OtBu. To a solution of Ac-Hel$_1$-OH (12.7 mg, 40.7 μmol, 1.0 equiv, prepared as described in the accompanying paper) in DMF (2 mL) at 0 °C under N_2 was added with stirring H-L-Ala-OtBu (46 μmol, 1.1 equiv) and HOBt (6.5 mg, 1.0 equiv), followed by DIEA (8.0 μL, 1.1 equiv) and EDMAPD (10.2 mg, 53.1 μmol, 1.3 equiv). After 1 h at 0 °C and 3 h at 23 °C the DMF was evaporated in vacuum, and the resulting residue was dissolved in CH_2Cl_2 (10 mL). The solution was extracted with 0.1 M HCl (3 × 3 mL), saturated $NaHCO_3$ (3 × 3 mL), brine (1 × 4 mL), then dried ($MgSO_4$), filtered, and evaporated to yield a crude solid (14.8 mg, 85%) which was purified by flash chromatography (19:1 $CHCl_3$/MeOH) to yield Ac-Hel$_1$-L-Ala-OtBu (13.8 mg, 80%) as an amorphous white solid: TLC R_f 0.60 (7:3 EtOAc/MeOH); ^{1}H NMR ($CDCl_3$, 300 MHz) δ 7.50, 6.35 (0.35 H, d, J = 7.4 Hz; 0.65 H, d, J = 8.1 Hz), 4.87, 4.68 (0.35 H, d, J = 8.5 Hz; 0.65 H, d, J = 9.1 Hz), 4.76, 4.50 (0.35 H, dd J = 2.5, 11.5 Hz; 0.65 H, d, J = 9.0 Hz), 4.44, 4.31 (0.65 H, qn, J = 7.3 Hz; 0.35 H, qn, J = 7.3 Hz), 4.39–4.29, 4.20–4.18 (0.65 H, m; 0.35 H, m), 3.97, 3.89, 3.83–3.74 (0.35 H, dd, J = 5.3, 10.3 Hz; 0.35 H, d, J = 10.3 Hz; 1.30 H, m), 3.18, 2.86 (0.65 H, dd, J = 5.1, 15 Hz; 0.35 H, dd, J = 4.4, 15 Hz), 2.84–2.70 (1 H, m), 2.58, 2.45 (0.65 H, d, J = 13.7 Hz; 0.35 H, d, J = 13.3 Hz), 2.46, 2.32 (0.35 H, dd, J = 1.5, 15 Hz; 0.65 H, dd, J = 9.9, 15 Hz), 2.17, 2.14 (1.95 H, s; 1.05 H, s), 2.16–1.91 (3 H, m), 1.82–1.69 (1 H, m), 1.46 (9 H, s), 1.39, 1.38 (1.05 H, d, J = 7.4 Hz; 1.95 H, d, J = 7.4 Hz); MS m/e 425 (M^+), 369 (M^+ – tBu), 352 (M^+ – OtBu), 325 (M^+ – CO_2tBu), 281 (M^+ – NHCHCH$_3$CO$_2$tBu), 253 (M^+ – CONHCHCH$_3$CO$_2$tBu); HRMS calcd for $C_{20}H_{31}N_3O_5S$ 425.1984, found 425.19842.

Assignment of Alanine NH Resonances for Ac-Hel$_1$-(L-Ala)$_n$-OtBu Conjugates by Synthesis and Study of Deuterated Ala Derivatives. Using the above protocols the following Ac-Hel$_1$-(L-Ala)$_n$-OtBu derivatives in which one or more Ala residues were replaced by NH-CD(CD$_3$)-CO residues were synthesized (Ala-d_4 is denoted by A, and Ac-Hel$_1$ and OtBu residues are omitted): A-A, A-A-A, A-A-A-A, A-A-A-A, A-A-A-A, A-A-A-A; A-A-A-A-A, A-A-A-A-A, A-A-A-A-A-A, A-A-A-A-A-A. The ^{1}H NMR spectra of these derivatives allowed unique assignment of all NH proton resonances for the di-, tri-, tetra-, and hexaAla derivatives. Chemical shift assignments for the pentaAla derivatives were made by analogy with the tetra and hexa derivatives.

NMR Studies. All spectra were obtained at 500 MHz on a Varian VXR500S spectrometer, with data processing on a SUN SPARC 1+ workstation using Varian VNMR 3.1 and 3.2 software. Difference NOE experiments[30] were run at 35.0 °C. Generally, 256 on- and off-resonance irradiated transients were collected in an interleaved fashion, employing a 3.5-s presaturation and a 1.0-s recycle delay. Line broadening (0.5 Hz) was applied to minimize Bloch–Siegert shifts.

All 2D spectra were run in the phase-sensitive mode, employing the method of States et al.[31] Resonance assignment of DMSO-d_6 was achieved by double-quantum filtered COSY experiments[32] run at 25.0 °C. Each hypercomplex data set comprised 200 increments of 32 scans each, containing 2048 points per scan and run with a recycle time of 6.0 s. This protocol provided a digital resolution in ω_2 of approximately 2.4 Hz/data points over the 4900-Hz spectra width. The free-induction decays were zero-filled to a final 2K × 1K data matrix and transformed with gaussian weighting in ω_2 and sine-bell weighting in ω_1. 500-MHz ROESY experiments[33] were performed in $DCDCl_3$ and DMSO-d_6 at 25.0 °C and in 3:1 DMSO-d_6/$CDCl_3$ at 5 °C using a pulsed spin lock[34] yielding an effective B_1 field strength of 3262 Hz during the 350-ms mixing period. The 30° mixing pulse was preceded and followed by a hard 90° pulse for resonance offset compensation. To identify spurious Hartmann–Hahn transfer peaks the ROESY spectra in DMSO-d_6/$CDCl_3$ were acquired with carrier frequency offsets varied by 200 Hz. Spectral widths were 5200–5600 Hz. For each hypercomplex data set, 32 scans of 240–512 increments were collected, with each incerement described by 2048 data points. The FIDs were zero-filled to a 2K × 1K data matrix and transformed with gaussian or shifted-gaussian weighting in ω_2 and with shifted gaussian or shifted sinebell weighting in ω_1. Spectral enhancement was gained in both ω_1 and ω_2 by means of a 5th order polynomial baseline correction.

Molecular Modeling. Energy minimization calculations were carried out on a Silicon Graphics Personal Iris minicomputer using the Quanta 2.1 version of CHARMm marketed by the Polygen Corp. In order to avoid uncertainties in torsional strain estimates, all torsional angles in the .RTF file were redefined to exclude hydrogen atoms at the terminal positions. Energies of defined conformations were minimized by a sequence involving steepest descents, followed by conjugate gradient, ending with the adopted basis Newton–Rafeson algorithm. The recommended charge for secondary amides of H (+0.14); N (–0.35); C (+0.55); and O (–0.55) were used. Total molecular charges were summed to zero by distributing surplus amide charge evenly over neighboring backbone atoms.

Appendix. Mass Action Expressions for Template-Based Helix Nucleation

In this section, mass action expressions are derived for the formation of templated helices. Any equilibrium involving n species can be characterized in terms of a linked sequence of $n - 1$ local equilibrium constants, each defining the relative stability of a pair of the n species. Although there are $n!/2$ ways of selecting these sequences, the

(30) Hall, L.; Sanders, J. *J. Am. Chem. Soc.* **1980**, *102*, 5703–5711.
(31) States, D. J.; Habekorn, R. A.; Ruben, D. J. *J. Magn. Res.* **1982**, *48*, 286–292.
(32) Rance, M.; Sorensen, O.; Bodenhausen, G.; Wagner, G.; Ernst, R.; Wuethrich, K. *Biochem. Biophys. Res. Commun.* **1983**, *117*, 479–485. Neuhaus, D.; Wagner, G.; Vasak, M.; Kagi, J.; Wuethrich, K. *Eur. J. Biochem.* **1985**, *151*, 257–273.
(33) Bothner-By, A.; Stephens, R. L.; Lee, J. *J. Am. Chem. Soc.* **1984**, *106*, 811–813. Bax, A.; Davis, D. *J. Magn. Res.* **1985**, *63*, 207–213.
(34) Kessler, H.; Griesinger, C.; Kerssebaum, R.; Wagmer, K.; Ernst, R. *J. Am. Chem. Soc.* **1987**, *109*, 607–609.

particular choice has no effect on the overall equilibrium calculation, and the experimentally or conceptionally simplest choice is usually taken. The model derived here is similar to others used for helix-coil equilibria,[1] but contains the simplifying feature that helices in short peptides are assumed to be nucleated only at a template that is in a nucleating conformation and to propagate outward from it until broken by a residue in a coil state. Thus, a particular residue can be in a helical state only if preceded by the helix-nucleating template or by another helical residue. The resulting series of local equilibria for a 4-amino acid peptide linked to a template T with nucleating T_h and nonnucleating T_c conformations is given by (1), and the corresponding mass action expression that relates the concentration of the coil species T_c-c-c-c-c to that of all species is given by (2).

The simplest workable assumption is that for a templated helix of reasonable length a series of equilibrium constants K_i within the helix converge to a limiting value which is the propagation constant that would be observed in an untemplated oligopeptide that is analyzed by conventional Zimm–Bragg methods under the same experimental conditions. For a peptide conjugate of arbitrary length, expression (2) can be transformed to (3), (3′), and (4) in which A and B are composites of equilibrium constants that characterize the peptide-template interphase. Inspection of the forms of (1) and (2) reveals that A and B must be positive and A must be greater than 1.

$$\begin{array}{l} T_c\text{—c—c—c—c} \overset{K_1}{\rightleftharpoons} T_h\text{—c—c—c—c} \overset{K_2}{\rightleftharpoons} \\ \quad\text{(cs)} \qquad\qquad\quad \text{(ts)} \\ T_h\text{—h—c—c—c} \overset{K_3}{\rightleftharpoons} T_h\text{—h—h—c—c} \overset{K_4}{\rightleftharpoons} \\ \quad (te_1) \qquad\qquad\quad (te_2) \\ T_h\text{—h—h—h—c} \overset{K_5}{\rightleftharpoons} T_h\text{—h—h—h—h} \\ \quad (te_3) \qquad\qquad\quad (te_4) \end{array} \quad (1)$$

$$(T_c + T_h)/T_c = 1 + K_1(1 + K_2(1 + K_3(1 + K_4(1 + K_5)))) \quad (2)$$

$$T_h/T_c = X_4 = K_1 + K_1K_2 + K_1K_2K_3(1 + K_4 + K_4K_5) \quad (3)$$

if $K_4 = K_5 \equiv s$, then

$$Th/Tc = X_4 = (K_1 + K_1K_2) + K_1K_2K_3(1 + s + s^2) \quad (3')$$

more generally, if $(K_1 + K_1K_2) \equiv A$ and $K_1K_2K_3 \equiv B$, then

$$X_n = A + B(1 + s + ... + s^{n-2}) \quad (4)$$

Although the above analysis implicitly includes the effects of entropic fraying from the distal end of the conjugate, it neglects other destabilizing end group effects. The concept of hydrogen bonding valence for an amino acid residue allows a simple analysis of end group anomalies. Regarding the conformational mobility of a given amino acid residue as largely defined by the state of the four hydrogen bonding valences (2 CO sites, 2 NH sites) of its two flanking amide residues, one sees that a residue with all four valences defined by hydrogen bonds within a helical structure is maximally defined conformationally. For an N-templated helical peptide of n residues bearing an ester at the C-terminus, $n - 4$ residues have a hydrogen bonding valence of 4, 1 has a valence of 3, 2 have a valence of 2, and 1 has a valence of 1. For an N-templated peptide bearing a secondary amide at its C-terminus, $n - 3$ residues have a valence of 4, 1 has a valence of 3, and 2 have a valence of 2. (It is important to note that once a helix has reached sufficient length to have structurally well-defined template interface, C-terminal, and core regions, additional residues only add to the length of the core, and the equilibrium constants s in expressions (3) and (4) in such cases apply primarily to core residues.)

Results from a comparison of the ϕ,ψ angles of amino acid residues of a short peptide that has been energy minimized by molecular modeling suggest that only the C-terminal residue shows significant deviations of ϕ and ψ angles. A survey of protein X-ray structural data shows that structural deviations are frequently noted in the last 2–4 residues at an α-helix C-terminus.[25] Almost certainly in some of these cases amino acid residues with helix-terminating roles[29] contribute to the deviations, which would be expected to be smallest for analogous homopeptides. Moreover it is important to distinguish between structure and energetics. A residue at the C-terminus of a helix flanked by amides with two helical NH hydrogen bonds but no helical CO hydrogen bonds may conceivably contribute a nearly normal s value to the state sum as defined from the N-terminus. The C-terminal end group effect thus may well be confined to a single amino acid residue.

Since the first two residues can be expected to respond to unusual features of the template-peptide interface and the last one or two may reflect end group anomalies, accurate estimations of s values for short peptides can only result from analysis of series of oligomers that extend to at least 6–8 amino acid residues. Since s values less than 0.7 result in highly frayed helices with average length shorter than this distance, calculations of s values in this range from homopeptide data have a large intrinsic uncertainty. Very large s values generate helices that are completely nucleated, with (t)/(c) ratios that are immeasurably large; again, a complete series of template–peptide conjugates cannot be studied, and only an approximate lower bound on s can be set.

The case of equal probability of c or h states at a given amino acid site corresponds to an s value of 1.0 and therefore to a $\Delta G° = 0$. Nevertheless $\Delta G°$ for the formation of a global helix made up of such residues is negative, owing to entropic stabilization. The source of this effect can be seen from the data of Table IA. Since s = 1.0, the coil conformer T_h-c_6, which offers each amino acid only a single choice of state, is in equilibrium with an equally abundant conformer in which the first residue is helical, T_h-hc_5. However, because the first amino acid residue of this conformer is helical, the second residue has two equally probable states availabe to it, h or c; the h state at the second residue now allows two equally probable states for the third residue, and the form of communication of structure thus arises only because of the condition that a preexisting helix greatly enhances the probability of its propagation. Propagation occurs despite the lack of a free energy difference between c and h states at any residue. If the process of counting helical states includes everything with an h state for the first amino acid residue, the resulting helix for a hexapeptide is six times more probable than the coil conformation.

The propagation term s thus can be used to describe two measurable properties of the helix, its overall stability and the degree to which it is conformationally well-defined. From Table IA it is apparent that only a helix with an s value considerably larger than 1.0 is present as a single helical conformation. We term short helices characterized by s values greater than 2–3 "robust", in that they are like simple organic structures that can be assigned a single conformation. By contrast, short helices characterized by s values of 0.7 to 1.5 are ensembles of all possible rapidly

equilibrating helical substates. We term such helices "frayed".

Acknowledgment. Financial support from Pfizer Research and from the National Science Foundation (Grant 8813429-CHE) is gratefully acknowledged. Mass specral data were provided by the MIT Mass Spectrometry Facility, which is supported by NIH Grant No. RR00317 (to K. Biemann).

Registry No. Ac-Hel$_1$-OH, 120980-87-2; H-Ala-OBu-*t*, 21691-50-9; Ac-Hel$_1$-Ala-OBu-*t*, 120980-91-8; Ac-Hel$_1$-Ala-OH, 119888-30-1; Ac-Hel$_1$-(Ala)$_2$-OBu-*t*, 119872-62-7; Ac-Hel$_1$-(Ala)$_2$-OH, 120980-92-9; Ac-Hel$_1$-(Ala)$_3$-OBu-*t*, 119872-63-8; Z-(Ala)$_2$-OBu-*t*, 13883-50-6; H-(Ala)$_3$-OBu-*t*, 65356-57-2; Ac-Hel$_1$-(Ala)$_4$-OBu-*t*, 119872-64-9; Z-(Ala)$_4$-OBu-*t*, 13883-53-9; H-(Ala)$_4$-OBu-*t*, 136088-66-9; Ac-Hel$_1$-(Ala)$_5$-OBu-*t*, 136088-67-0; Ac-Hel$_1$-(Ala)$_6$-OBu-*t*, 136088-68-1; H-Sar-OBu-*t*-HCl, 136088-69-2; Ac-Hel$_1$-Sar-OBu-*t*, 136088-70-5; Ac-Hel$_1$-Sar-OH, 136088-71-6; H-Ala-OBu-*t*-HCl, 13404-22-3; Ac-Hel$_1$-Sar-Ala-OBu-*t*, 136088-72-7; Ac-Hel$_1$HSar-(Ala)$_4$-OBu-*t*, 136088-73-8; Ac-Hel$_1$-OMe, 119888-29-8; Ac-Hel$_1$-OBu-*t*, 136088-74-9; Ac-Hel$_1$-(Ala)$_3$-NHMe, 136088-75-0; Ac-Hel$_1$-(Ala-d_3)-(Ala-d_4)$_2$-Ala-OBu-*t*, 136088-76-1; Ac-Hel$_1$-(Ala)$_2$-NHMe, 136088-77-2; Ac-Hel$_1$-(Ala)$_6$-NHMe, 136088-78-3.

Supplementary Material Available: Details of solvent purification, synthesis and characterization of higher alanine homologues of Ac-Hel$_1$-L-Ala-OH, and sarcosine conjugates (9 pages). Ordering information is given on any current masthead page.

A New Procedure for the Conversion of Thiols into Reactive Sulfenylating Agents[1]

D. H. R. Barton, R. H. Hesse,* A. C. O'Sullivan,† and M. M. Pechet

Research Institute for Medicine and Chemistry, 49 Amherst Street, Cambridge, Massachusetts 02142

Received April 12, 1991

Thiols may be converted in high yield into unsymmetrical 2-pyridyl disulfides **3**. Treatment of these with alkylating agents (e.g., alkyl fluorosulfonates or oxonium salts) affords the corresponding *N*-alkylpyridyl disulfides **4**, which are potent sulfenylating agents (Scheme II) and react smoothly with a variety of sulfur nucleophiles (e.g., thiols, thiones, thioamides, dithiocarbamates, thiocyanate, etc.) to afford disulfides, with amines to afford sulfenamides, and with β-diketones to afford sulfides. This new method is particularly well-suited to the preparation of unsymmetrical disulfides and sulfenamides from complex and otherwise reactive thiols.

We were interested in the possibility that unsymmetrical disulfides derived from sulfur-containing drugs might serve as useful "prodrugs". There is, however, currently no convenient *general* method for the conversion of a thiol into a *reactive* sulfenylating agent as a prelude to formation of unsymmetrical disulfides,[2] sulfenamides, sulfides, etc., and thus such sulfenylating agents are normally secured through a variety of indirect methods.[3] The crucial limitation upon the direct approach stems from the tendency of unreacted thiol to react with the sulfenylating agent as it is formed, affording symmetrical disulfide (Scheme I).

Scheme I

$$\mathrm{RSH} \xrightarrow[\text{slow}]{} \mathrm{RSX} \xrightarrow[\text{fast}]{\mathrm{RSH}} \mathrm{RSSR}$$

We now report a rather general procedure for conversion of thiols into reactive sulfenylating agents that skirts the above limitation through conversion of the thiol into a *latent* sulfenylating agent that is then "activated" in a second step *in the absence of thiol*. Specifically, the thiol is converted into an unsymmetrical 2-pyridyl disulfide (Scheme IIa) **3**, which is activated through N-alkylation into **4** (Scheme IIb).

The *N*-alkylpyridinium disulfides **4** are potent sulfenylating agents and react at sulfur with various nucleophiles (Scheme IIc) driven by extrusioon of 1-alkyl-2-thiopyridone (**5**). (The reactivity of **5** as a leaving group has been

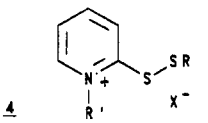

4

	R	R'	X
a)	R_C	Me	FSO_3^-
b)	"	Et	PF_6^-
c)	"	Me	$CF_3SO_3^-$
d)	Me	Et	BPh_4^-
e)	"	Et	FSO_3^-

(R_C = cholest-5-en-3β-yl)

foreshadowed by the various reactions driven through the departure of 1-alkyl-2-pyridone.[4]) The unsymmetrical disulfides **3** can be made quite simply through reaction of a thiol with 2,2′-dipyridyl disulfide (**2**, X = 2-thiopyridyl), a reagent that is commercially available[5] and that has been

* Author to whom correspondence should be addressed.
† Present address: Ciba-Geigy AG, 4002 Basel, Switzerland.

(1) Taken in part from the Ph.D. Thesis (London University) of A. C. O'Sullivan.

(2) Among the various methods, the one promising to be most general lies in conversion of a thiol into a sulfenyl hydrazide through reaction with diethyl azodicarboxylate: Mukalyama, T.; Takahashi, K. *Tetrahedron Lett.* **1968**, 5907. Bockelhelde, V., Mindt, J. L. *Ibid.* **1970**, 1203. However, see: Helmer, N. E.; Field, L. *J. Org. Chem.* **1970**, *35*, 3012. Field, L.; Hanley, W. S.; McVeigh, I. *Ibid.* **1971**, *36*, 2735.

(3) For reviews see: Kühle, E. *The Chemistry of the Sulfenic Acids*; G. Thieme: Stuttgart, 1973. Hogg, D. R. In *Comprehensive Organic Chemistry*; Barton, D. H. R., Ollis, W. D., Eds.; Pergamon: Oxford, 1979; Vol. 3, pp 261ff. Field, L. In *The Organic Chemistry of Sulfur*; Oae, S., Ed.; Plenum: New York, 1977; Chapter 7, pp 303ff.

0022-3263/91/1956-6697$02.50/0